

Supporting Information

**Histidine-conjugated DNA as an Intriguing Biomolecular
Depot for Metal Ions**

Soyoung Park,,¹Haruka Matsui, Koyuki Fukumoto, Ji Hye Yum and Hiroshi
Sugiyama*,^{1,2}*

¹Department of Chemistry, Graduate School of Science, Kyoto University, Kitashirakawa-
oiwakecho, Sakyo-ku, Kyoto 606-8502, Japan

²Institute for Integrated Cell-Material Sciences (iCeMS), Kyoto University, Yoshida-
ushinomiya-cho, Sakyo-ku, Kyoto 606-8501, Japan

**Corresponding author:* Dr. Soyoung Park, Prof. Dr. Hiroshi Sugiyama

Tel.: (+)81-75-753-4002; Fax: (+)81-75-753-3670

E-mail: oleesy@kuchem.kyoto-u.ac.jp, hs@kuchem.kyoto-u.ac.jp (H.S.)

Table of contents

1. Materials
2. Methods and Equipment
3. **Scheme S1**: Synthetic Route of the Incorporated Organic Compounds
4. Synthesis and characterization of amino acid-conjugated D-threoninol backbone
 - **Figure S1-S4**: NMR and Mass Data of Newly Synthesized Compounds (**2a-2d**)
5. **Table S1**: Analytical HPLC Profile of Artificial ODN
6. **Table S2**: MALDI-TOF-Mass Data of Artificial ODNs
7. UV-melting
 - **Figure S5**: UV-melting curve and T_m value graph of **ODN 1/ODN 2 (Y)** with Cu^{2+}
 - **Figure S6**: UV-melting curve and T_m value graph of **ODN 3/ODN 4 (Y)** with Cu^{2+}
 - **Figure S7**: UV-melting curve and T_m value graph of **ODN 14/ODN 15** with Cu^{2+}
 - **Figure S8**: UV-melting curve and T_m value graph of **ODN 1/ODN 2 (His)** with metal ions
 - **Figure S9**: UV-melting curve and T_m value graph of **ODN 1/ODN 2 (His)** with Cu^{2+}
 - **Figure S10**: UV-melting curve and T_m value graph of **ODN 1/ODN 2 (His)** with Zn^{2+}
 - **Figure S11**: UV-melting curve and T_m value graph of **ODN 1/ODN 2 (His)** with Ni^{2+}
 - **Figure S12**: UV-melting curve and T_m value graph of **ODN 16/ODN 17** with Cu^{2+}
 - **Figure S13**: UV-melting curve and T_m value graph of **ODN 5/ODN 6** with metal ions
 - **Figure S14**: UV-melting curve and T_m value graph of **ODN 5/ODN 6** with Cu^{2+}
 - **Figure S15**: UV-melting curve and T_m value graph of **ODN 5/ODN 6** with Zn^{2+}
 - **Figure S16**: UV-melting curve and T_m value graph of **ODN 5/ODN 6** with Ni^{2+}
 - **Figure S17**: UV-melting curve and T_m value graph of **ODN 10/ODN 11** with metal ions
 - **Figure S18**: UV-melting curve and T_m value graph of **ODN 12/ODN 13** with metal ions
 - **Figure S19**: UV-melting curve and T_m value graph of **ODN 20/ODN 21** with metal ions
 - **Figure S20**: UV-melting curve and T_m value graph of **ODN 22/ODN 23** with metal ions

Table of contents

8. CD spectroscopy

- **Figure S21:** CD spectra of the duplexes **ODN 1/ODN 2 (Y)** with Cu^{2+}
- **Figure S22:** CD spectra of the duplexes **ODN 3/ODN 4 (Y)** with Cu^{2+}
- **Figure S23:** CD spectra of the duplexes **ODN 1/ODN 2 (His)** with metal ions
- **Figure S24:** CD spectra of the duplexes **ODN 1/ODN 2 (His)** with Cu^{2+}
- **Figure S25:** CD spectra of the duplexes **ODN 1/ODN 2 (His)** with Zn^{2+}
- **Figure S26:** CD spectra of the duplexes **ODN 1/ODN 2 (His)** with Ni^{2+}
- **Figure S27:** CD spectra of the duplexes **ODN 16/ODN 17** with Cu^{2+}
- **Figure S28:** CD spectra of the duplexes **ODN 5/ODN 6** with metal ions
- **Figure S29:** CD spectra of the duplexes **ODN 5/ODN 6** with Cu^{2+}
- **Figure S30:** CD spectra of the duplexes **ODN 5/ODN 6** with Zn^{2+}
- **Figure S31:** CD spectra of the duplexes **ODN 1/ODN 2 (His)** with Ni^{2+}
- **Figure S32:** CD spectra of the duplexes **ODN 10/ODN 11** with metal ions²⁺
- **Figure S33:** CD spectra of the duplexes **ODN 12/ODN 13** with metal ions²⁺
- **Figure S34:** CD spectra of the duplexes **ODN 20/ODN 21** with metal ions²⁺
- **Figure S35:** CD spectra of the duplexes **ODN 22/ODN 23** with metal ions²⁺

9. Asymmetric Diels-Alder Reactions Catalyzed by DNA-based Hybrid Catalysts

- **Figure S36.** HPLC analysis of the asymmetric Diels-Alder reaction

10. ABTS Oxidative Reaction Catalyzed by Quadruplex-Duplex Hybrids

- **Figure S37:** Equation for the calculation of V_o value of ABTS oxidative reaction
- **Figure S38:** pH dependency of ABTS oxidative reaction
- **Figure S39:** Fast optimization of ABTS oxidative reaction on 96 plate

11. Molecular Modeling Studies

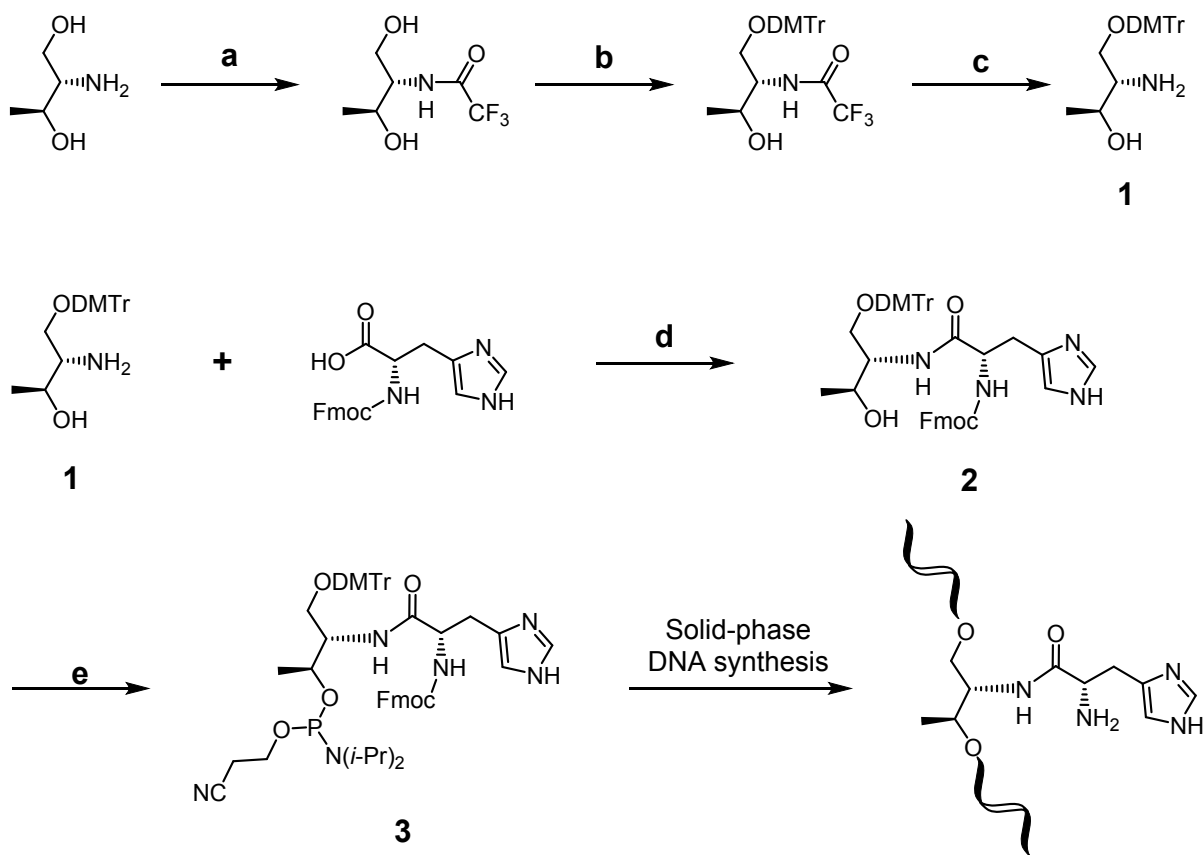
- **Figure S40:** Molecular modeling of the duplex histidine-conjugated oligonucleotides
- **Figure S41:** Molecular modeling of quadruplex-duplex histidine-conjugated oligonucleotides

Materials

N,N-Dimethylformamide dimethyl acetal, potassium phthalimide, 4,4'-dimethoxytrityl chloride, triethylamine, *N,N*-dimethyl-4-aminopyridine, 3-chloro-1-propanol, 3-amino-1-propanol were received from Wako Chemicals and used without further purification. 2-cyanoethyl *N,N*-diisopropylchloro phosphoramidite, D-threoninol (97%), hydrazine monohydrate, 2,2'-bipyridine-5,5'-dicarboxylic acid, 4-amino-1-butanol were purchased from Sigma-Aldrich Chemicals Co. and used as received. *N,N*-Diisopropylethylamine was purchased from Nacalai and used as received. 6-Amino-1-hexanol, 6-chloro-1-hexanol were obtained from TCI. Glen-Pak™ DNA and RNA cartridges columns are purchased at Glen research and used. All other chemicals and solvents were purchased from Sigma-Aldrich Chemicals Co., Wako Pure Chemical Ind. Ltd., TCI, or Kanto Chemical Co. Inc. and used without further purification and synthetic oligonucleotides were obtained from Sigma Genosys. Water was deionized (specific resistance of ≥ 18.0 MW cm at 25°C) by a Milli-Q system (Millipore Corp.).

Methods and Equipment

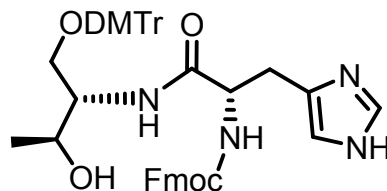
NMR spectra were obtained on a JEOL JNM ECA-600 spectrometer operating at 600 MHz for ^1H NMR and 150 MHz for ^{13}C NMR in CDCl_3 unless otherwise noted. Flash column chromatography was performed employing Silica Gel 60 (70–230 mesh, Merck Chemicals). Silica-gel preparative thin-layer chromatography (PTLC) was performed using plates from Silica gel 70 PF₂₅₄ (Wako Pure Chemical Ind. Ltd.). Enantiomeric excess (*ee*) determinations were performed by HPLC analysis (Chiralcel AD-H, OD-H) using UV-detection. DNA concentrations were measured by Nanodrop ND-1000 spectrophotometer. Rotary mixing of reaction suspension was performed by Intelli-Mixer RM-2 (Elmi).

Scheme S1. Synthetic Route of the Incorporated Organic Compounds

Reagents and conditions: (a) $\text{CF}_3\text{COOC}_2\text{H}_5$, dry MeOH, 0°C , 2 h ; (b) DMT-Cl, DIEA, DMAP, CH_2Cl_2 , pyridine, $0^\circ\text{C} \rightarrow \text{r.t.}$ 2.5 h; (c) NH_3 , EtOH/ H_2O , r.t. 3 days ; (d) PyBOP, DIEA, DMF, r.t., 1 day. ; (e) $(i\text{Pr}_2\text{N})_2\text{PO}(\text{CH}_2)_2\text{CN}$, DIEA, CH_3CN , $0^\circ\text{C} \rightarrow \text{r.t.}$ 1.5 h

Synthesis and characterization of amino acid-conjugated D-threoninol backbone

Figure S1. Histidine-conjugated D-threoninol backbone (2a)



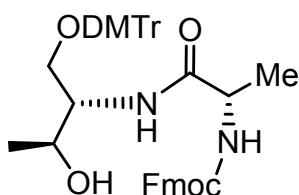
(2*S*)-2-(9*H*-fluoren-9-ylmethoxycarbonylamino)-3-[1-(9*H*-fluoren-9-ylmethoxycarbonyl)imidazol-4-yl]propane-carboxamide *N*-((2*S*,3*S*)-1-({4,4'-dimethoxytrityl-oxy})-3-hydroxybutan-2-ol)

Detail synthetic route for DMTr-protected Dthreoninol backbone (**1**) is written on the previous report by Asanuma, H. and his co-workers.^{S1} To DMF solution (20 mL) containing Fmoc-His-OH (377 mg, 1.0 mmol), PyBOP (520 mg, 1.0 mmol), and DIEA (0.7 mL) was added DMF solution (5 mL) of compound **1** (489 mg, 1.2 mmol). Then the resulting reaction mixture was stirred at room temperature for 1 day. After the precipitate was removed by filtration, the filtrate was evaporated and the obtained solid was subjected to silica gel column chromatography (CH₂Cl₂ MeOH = 30:1) to afford 311 mg (0.41 mmol) of the product (yield, 41%).

¹H NMR ((CD₃)₂CO): δ 7.83 (d, *J* = 7.1 Hz, 2H), 7.67 (d, *J* = 7.7 Hz, 1H), 7.61 (m, 2H), 7.48-7.45 (m, 2H (1H+NH)), 7.38 (t, *J* = 7.7 Hz, 2H), 7.33-7.26 (m, 8H), 7.16 (t, *J* = 7.1 Hz, 1H), 7.03 (d, 6.5 Hz, 1H (NH)), 6.93 (s, 1H), 6.84 (d, *J* = 8.3 Hz, 4H), 4.54 (d, *J* = 5.9, 1H), 4.27 (m, 2H), 4.19 (t, *J* = 7.1 Hz, 1H) 4.08 (t, *J* = 5.1 Hz, 1H), 4.01 (q, *J* = 4.6 Hz, 1H), 3.72 (s, 3H), 3.71 (s, 3H),

3.24 (dd, $J = 8.6, 5.1$ Hz, 1H), 3.13-3.05 (m, 3H), 1.01 (d, $J = 6.5$ Hz, 3H). ^{13}C NMR ($(\text{CD}_3)_2\text{CO}$): d 172.09, 159.47, 156.83, 146.24, 145.17, 144.89, 142.04, 142.00, 136.94, 136.92, 135.97, 130.94, 130.91, 129.00, 128.53, 128.49, 127.97, 127.41, 126.25, 126.16, 120.74, 113.83, 86.70, 67.37, 67.17, 64.27, 56.32, 56.04, 55.44, 47.94, 31.20, 20.60. HRMS (ESI-TOF) calculated for $\text{C}_{46}\text{H}_{46}\text{N}_4\text{NaO}_7$ $[\text{M}+\text{Na}]^+$ 789.3259, found 789.3259.

Figure S2. Alanine-conjugated D-threoninol backbone (2b)

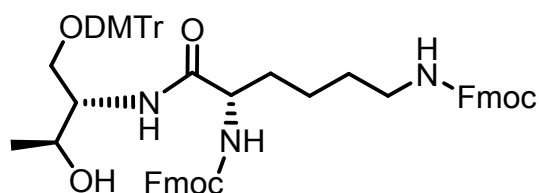


(2*S*)-2-(9*H*-fluoren-9-ylmethoxycarbonylamino)propane-carboxamide *N*-((2*S*,3*S*)-1-({4,4'-dimethoxytrityl-oxy})-3-hydroxybutan-2-ol)

^1H NMR ($(\text{CD}_3)_2\text{CO}$): δ 7.85 (d, $J = 7.7$ Hz, 2H), 7.70 (d, $J = 7.7$ Hz, 1H), 7.61 (d, $J = 7.1$ Hz, 1H), 7.46 (d, $J = 7.7$ Hz, 2H), 7.39 (td, $J = 7.1$ Hz, 3.4 Hz, 2H), 7.33-7.27 (m, 9H), 7.18 (t, $J = 7.4$ Hz, 1H), 6.86 (d, $J = 8.3$ Hz, 4H), 4.33-4.29 (m, 2H), 4.27-4.24 (m, 1H), 4.19 (t, $J = 7.1$ Hz, 1H), 4.10 (s (br), 1H), 4.01 (s (br), 1H), 3.77 (d, $J = 4.8$ Hz, 1H), 3.74 (d, $J = 3.0$ Hz, 6H), 3.25 (dd, $J = 8.0$ Hz, 6.2 Hz, 1H), 3.12 (dd, $J = 8.9$ Hz, 5.9 Hz, 1H), 1.40 (d, $J = 7.13$ Hz, 3H), 1.08 (d, $J = 6.5$ Hz, 3H). ^{13}C NMR (CDCl_3): d 172.68, 158.67, 155.99, 144.45, 143.75, 141.31, 135.41, 129.98, 128.03, 127.77, 127.15, 127.06, 125.15, 120.02, 113.37, 86.80, 68.31, 67.14, 64.89 (overlapped), 55.24,

53.57, 47.14, 19.93, 19.25. HRMS (ESI-TOF) calculated for $C_{43}H_{44}N_2NaO_7$ $[M+Na]^+$ 723.3000, found 723.3040.

Figure S3. Lysine-conjugated D-threoninol backbone (2c)

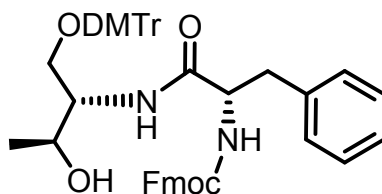


(2*S*)-6-amino-2-(9*H*-fluoren-9-ylmethoxycarbonylamino)hexane-carboxamide *N*-((2*S*,3*S*)-1-({4,4'-dimethoxytrityl-oxy})-3-hydroxybutan-2-yl)

1H NMR ($(CD_3)_2CO$): δ 7.84 (d, $J = 7.8$ Hz, 4H), 7.69 (d, $J = 7.8$ Hz, 1H), 7.66 (d, $J = 7.2$ Hz, 2H), 7.61 (t, $J = 7.8$ Hz, 2H), 7.46 (d, $J = 7.8$ Hz, 2H), 7.39 (t, $J = 7.5$ Hz, 2H), 7.38 (t, $J = 7.2$ Hz, 2H), 7.33-7.25 (m, 10H) 7.17 (t, $J = 7.5$ Hz, 2H), 7.13 (d, $J = 8.4$ Hz, 1H), 6.85 (d, $J = 7.2$ Hz, 4H), 6.70 (d, $J = 7.8$ Hz, 1H), 6.50 (t, $J = 5.1$ Hz, 1H), 4.34-4.24 (m, 4H), 4.20-4.16 (m, 2H), 4.09 (br, 1H), 4.03 (br, 1H), 3.77 (d, $J = 4.2$ Hz, 1H), 3.73 (d, $J = 3.6$, 6H), 3.25 (dd, $J = 8.4, 6.0$, 1H), 3.16 (q, $J = 4.2$ Hz, 1H), 3.12 (dd, $J = 9.0, 5.4$, 1H), 1.92 (m, 1H), 1.77-1.71 (m, 1H), 1.61-1.44 (m, 3H), 1.08 (d, $J = 6.0$ Hz, 3H). ^{13}C NMR ($CDCl_3$): d 171.79, 158.59, 156.65, 156.19, 144.31, 143.93, 143.89, 143.63, 141.25, 135.53, 135.29, 128.92, 129.86, 127.98, 127.90, 127.67, 127.61, 127.04, 126.99, 125.06, 124.97, 119.90, 113.27, 86.70, 68.21, 67.09, 66.54, 64.79, 55.14, 54.97, 53.68, 47.21, 47.06, 40.23, 32.31, 29.41, 22.32, 20.02. HRMS (ESI-TOF) calculated for $C_{61}H_{61}N_3NaO_9$

$[M+Na]^+$ 1002.4300, found 1002.4295.

Figure S4. Phenylalanine-conjugated D-threoninol backbone (2d)



(2*S*)-2-(9*H*-fluoren-9-ylmethoxycarbonylamino)-3-phenylpropanane-carboxamide *N*-((2*S*,3*S*)-1-({4,4'-dimethoxytrityl-oxy})-3-hydroxybutan-2-ol)

$^1\text{H NMR}$ ($(\text{CD}_3)_2\text{CO}$): δ 7.83 (d, $J = 7.7$ Hz, 2H), 7.61 (d, $J = 7.7$ Hz, 1H), 7.53 (d, $J = 7.7$ Hz, 1H),

7.46 (d, $J = 8.3$ Hz, 1H), 7.39-7.36 (m, 2H), 7.33 (d, $J = 7.7$ Hz, 6H), 7.29-7.23 (m, 6H),

7.20-7.16 (m, 3H (2H+NH)), 6.85 (d, $J = 7.1$ Hz, 4H), 6.79 (br, 1H (NH)), 4.60 (d, $J = 7.7$ Hz, 1H),

4.21 (t, $J = 9.2$ Hz, 1H), 4.15 (t, $J = 8.6$, 1H), 4.10 (t, $J = 7.1$ Hz, 2H), 3.73 (s, 3H), 3.72 (s, 3H),

3.27-3.22 (m, 2H), 3.13 (t, $J = 7.1$ Hz, 1H), 2.99 (dd, $J = 12.5, 9.5$ Hz, 1H), 1.02 (d, $J = 6.5$ Hz,

3H). $^{13}\text{C NMR}$ ($(\text{CD}_3)_2\text{CO}$): d 172.19, 159.49, 156.83, 146.29, 145.10, 144.85, 142.01, 141.99,

138.82, 136.98, 130.93, 130.26, 129.09, 128.99, 128.54, 128.48, 127.94, 127.42, 127.26, 126.20,

126.16, 120.73, 113.85, 86.76, 67.33, 66.76, 64.26, 57.49, 55.44, 55.36, 47.88, 39.08, 20.70.

HRMS (ESI-TOF) calculated for $\text{C}_{49}\text{H}_{48}\text{N}_2\text{NaO}_7$ $[M+Na]^+$ 799.3354, found 799.3340.

Preparation of phosphoramidite 2a-2d

DMT-protected amino acid derivative (0.5 mmol 1.0 equiv) was dissolved in 5 mL of dry dichloromethane. *N,N*-diisopropylethylamine (1.5 mmol, 3.0 equiv) and 2-cyanoethyl *N,N*-diisopropylchlorophosphoramidite (1.0 mmol, 2.0 equiv) were successively added to the solution at 0 °C, and the reaction mixture was stirred 1 h at RT. All volatiles were then evaporated and without further purification the residue dissolved in MeCN (1.5 mL) for DNA solid synthesis.

Oligonucleotide Synthesis

ODNs were synthesized on solid supports using triethylene glycol or propyl (octyl) linker-derived phosphoramidites and commercially available O^5' -dimethoxytrityl $-2'$ -deoxyribonucleoside O^3' -phosphoramidites. Solid-phase oligonucleotide synthesis was performed on an ABI DNA synthesizer (Applied Biosystem, Foster City, CA). The modified phosphoramidite was chemically synthesized as described above and without purification incorporated into oligonucleotide through coupling reaction for 10 minutes. Coupling yields linker-derived phosphoramidites were equal to the ones obtained with standard phosphoramidite building blocks. Cleavage from the solid support and deprotection were accomplished with 50:50 of MeNH₂ in 40 wt. % in water and NH₃ in 28 wt. % in water at rt for 15 min and then at 65 °C for 15 min. Elution is applied to Glen-Pak™ DNA and RNA cartridges columns and the purification steps are performed followed by the procedures. Final elution is undergone normal-phase HPLC purification (The purification conditions shown with HPLC chart). After purification by HPLC, products were confirmed by MALDI-TOF MS (Table S2). DNA concentrations were determined by using the Nano drop ND-1000 (Nano-drop Technologies, Wilmington, DE).

Table S1. Analytical HPLC Profile of Artificial ODN

For HPLC analysis, COSMOSIL 5C18 AR-II (Nacalai Tesque, Inc., Kyoto, 150 × 10 mm id), a linear gradient of 3 to 30% acetonitrile over 30 min at a flow rate of 3.0 mL/min. 50 mM ammonium formate (pH 6.6) was used as a buffer on 254 nm.

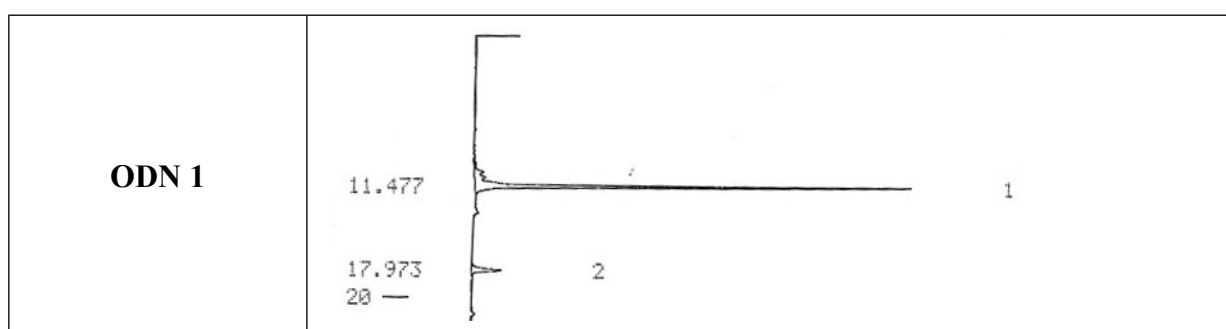


Table S2. MALDI-TOF-Mass data of ODNs.

Name	DNA oligomers	Calcd.	Found.
ODN 1	5'-GCATGG- His -CACGGT-3'	3989.75	3990.30
ODN 2 (His)	5'-ACCGTG- His -CCATGC-3'	3909.73	3909.68
ODN 3	5'-GCATGA- His -TACGGT-3'	3988.75	3988.50
ODN 4 (His)	5'-ACCGTA- His -TCATGC-3'	3908.74	3908.42
ODN 5	5'-GCATGG- His - His -CACGGT-3'	4293.84	4293.57
ODN 6	5'-ACCGTG- His - His -CCATGC-3'	4213.83	4213.85
ODN 7	5'-GCATGA- His - His -TACGGT-3'	4292.84	4291.62
ODN 8	5'-ACCGTA- His - His -TCATGC-3'	4212.83	4213.18
ODN 9	5'- GG - His - His - GG -3'	1863.36	1861.87
ODN 10	5'- GG - His - His - GG CGCGAAG-3'	4055.77	4053.96
ODN 11	5'-CTTCGCG GG - His - His - GG -3'	3997.72	3996.20
ODN 12	5'- GG - Ala - His - GG CGCGAAG-3'	3989.71	3987.10
ODN 13	5'-CTTCGCG GG - Ala - His - GG -3'	3931.65	3931.50
ODN 20	5'-GCATGG- Lys -CACGGT-3'	3980.78	3978.94
ODN 21	5'-ACCGTG- Lys -CCATGC-3'	3900.74	3898.50
ODN 22	5'-GCATGG- Phe -CACGGT-3'	3999.75	3999.08
ODN 23	5'-ACCGTG- Phe -CCATGC-3'	3919.74	3920.29

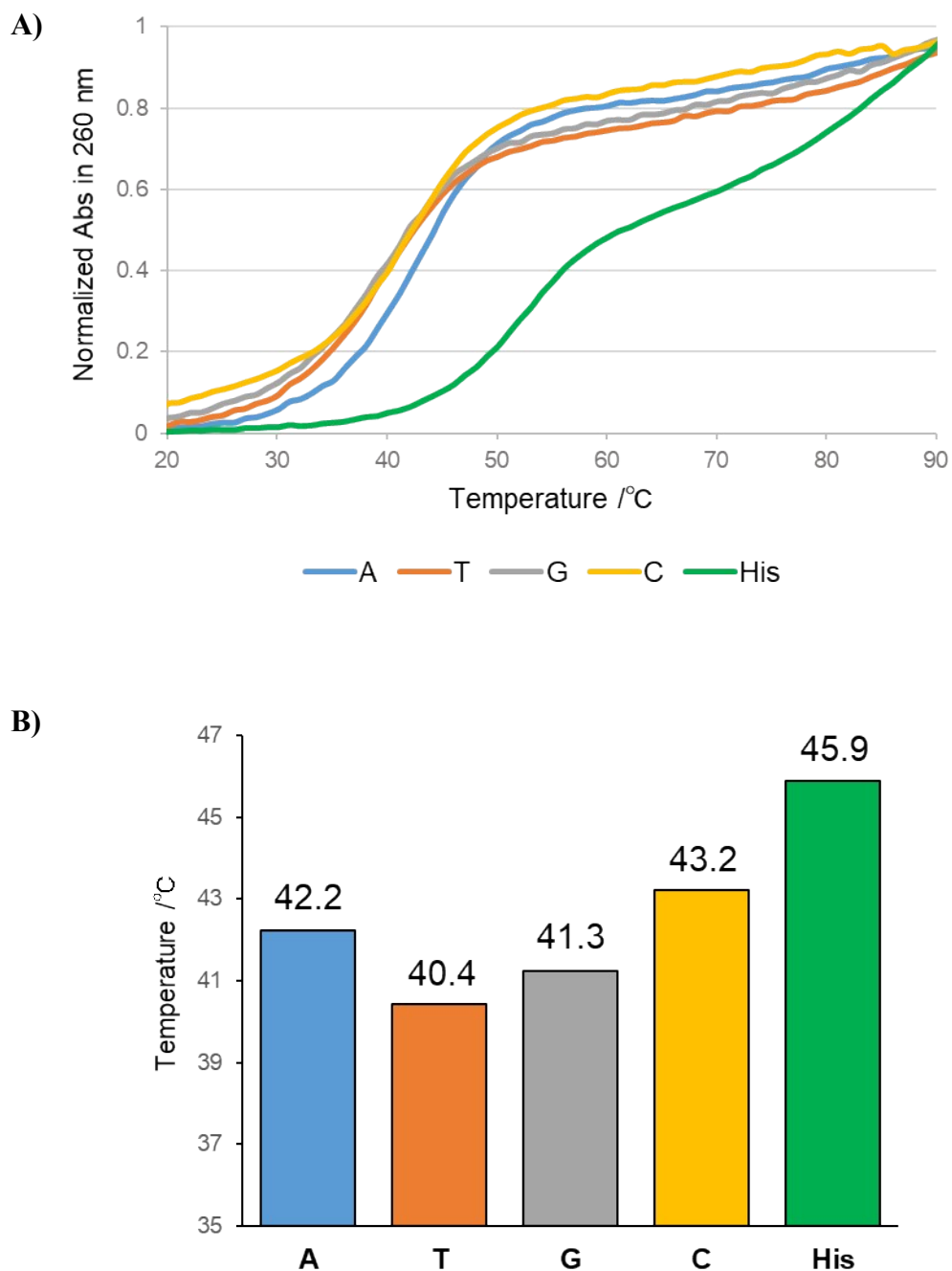
Other DNA oligomers were purchased from Sigma Genosys.

UV-melting

Melting temperature was determined by measuring changes in absorbance at 260 nm as a function of temperature using a JASCO V-650 UV/VIS spectrophotometer. JASCO PAC-743R equipped with a high-performance temperature controller and micro auto eight-cell holder. Absorbance was recorded in the forward and reverse direction at temperatures from 5 to 95 °C at a rate of 1 °C/min. The melting samples were denatured at 95 °C for 4 min and annealed slowly to RT then stored at 5 °C until experiments were initiated. All melting samples were prepared in a total volume of 150 ml containing 2.5 μM of each duplex forming oligonucleotides, 2.5 μM Cu(NO₃)₂, (ZnCl₂, NiCl₂, and FeCl₃), 20 mM MOPS buffer (pH 6.5) and 100 mM NaCl. Or 7.0 μM of each quadruplex-duplex forming oligonucleotides, 6.7 μM Cu(NO₃)₂, (ZnCl₂, NiCl₂, CoCl₂, and FeCl₃), 20 mM Tris-HCl buffer (pH 7.4) and 100 mM KCl. All the experiments are duplicated (reproducibility of ±5%) and T_m values are calculated by averaging values.

Figure S5. Melting curves and T_m values of the duplexes ODN 1/ODN 2 (Y) in the presence of 1 equivalent of Cu^{2+} ^a

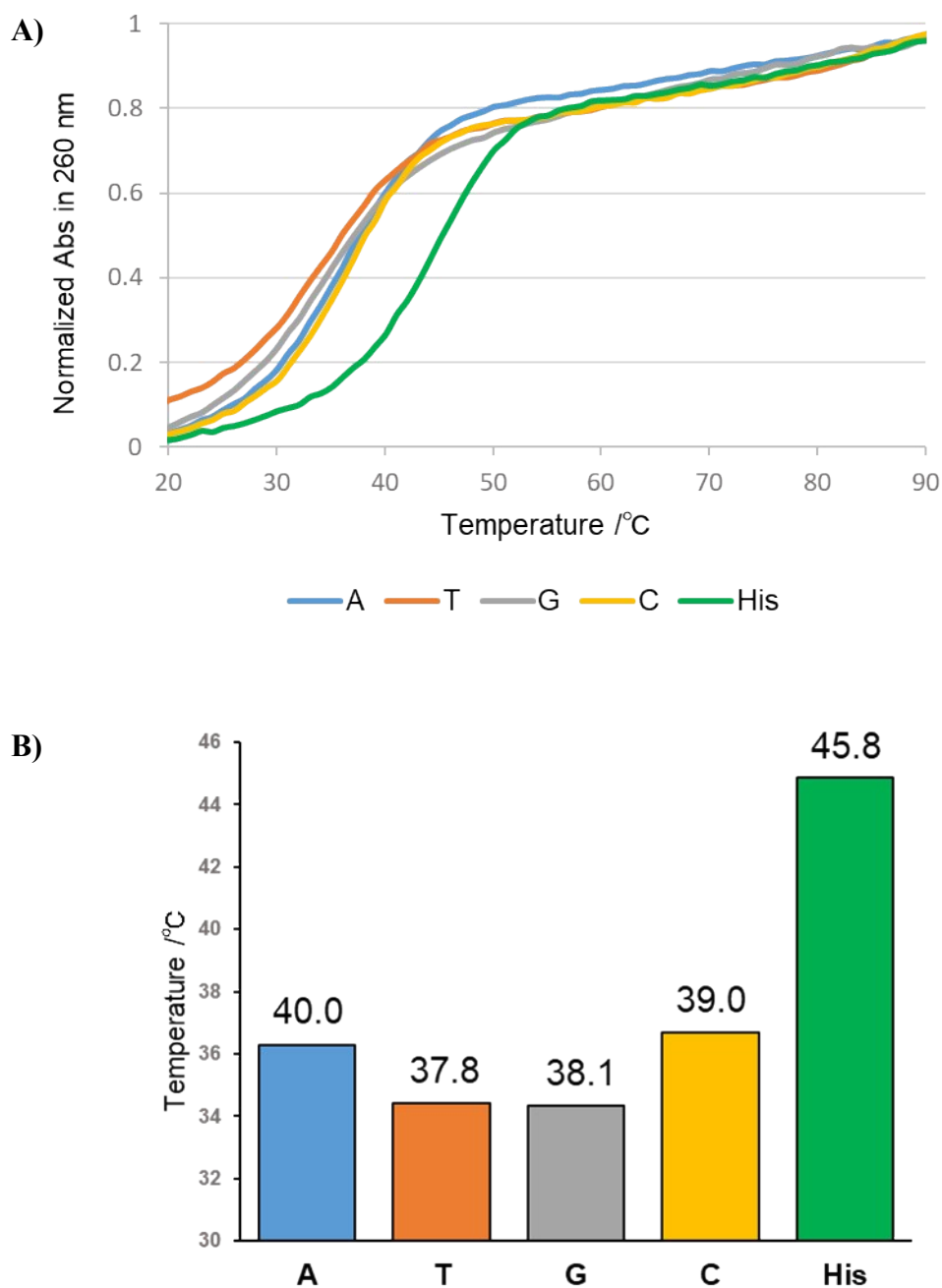
^a Solution conditions: 2.5 μM each DNA, 2.5 μM $\text{Cu}(\text{NO}_3)_2$ and 100 mM NaCl in 20 mM MOPS buffer (pH 6.5).



A) UV-melting curve of the duplexes ODN 1/ODN 2 (Y), B) T_m value graph of the duplexes ODN 1/ODN 2 (Y).

Figure S6. Melting curves and T_m values of the duplexes ODN 3/ODN 4 (Y) in the presence of 1 equivalent of Cu^{2+} ^a

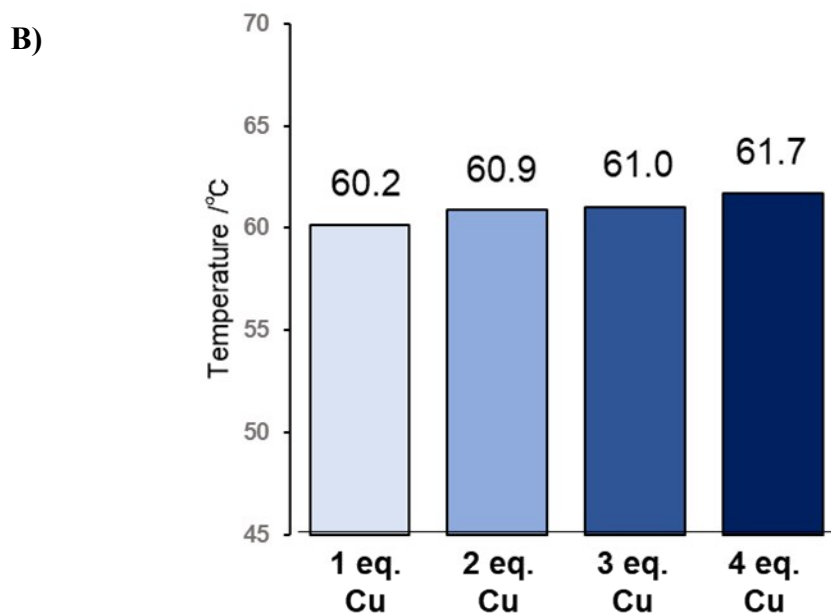
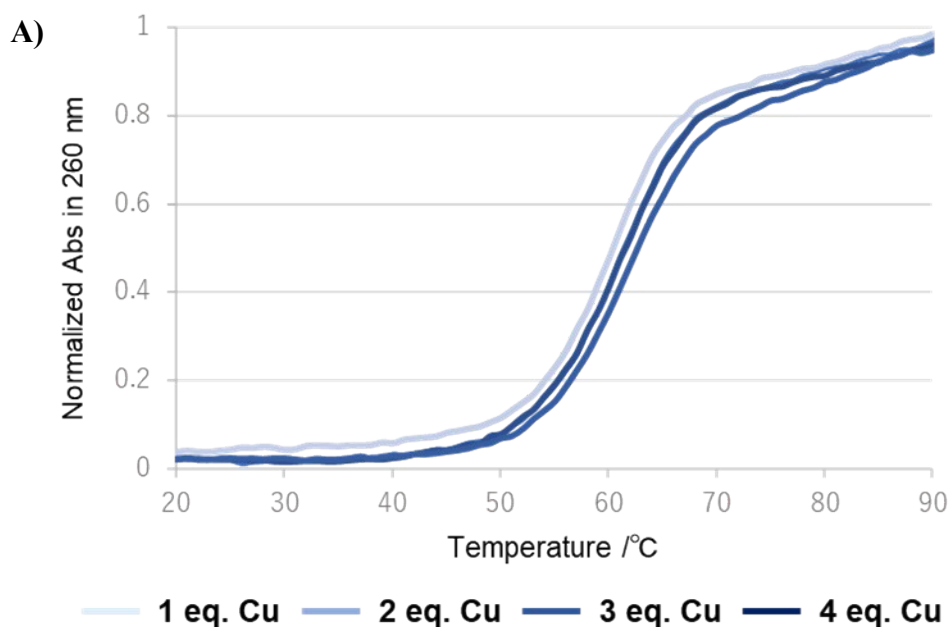
^a Solution conditions: 2.5 μM each DNA, 2.5 μM $\text{Cu}(\text{NO}_3)_2$ and 100 mM NaCl in 20 mM MOPS buffer (pH 6.5).



A) UV-melting curve of the duplexes **ODN 3/ODN 4 (Y)**, B) T_m value graph of the duplexes **ODN 3/ODN 4 (Y)**.

Figure S7. Melting curves and T_m values of the duplexes ODN 14/ODN 15 in the presence of 1-4 equivalent of Cu^{2+} ^a

^a Solution conditions: 2.5 μM each DNA, 2.5 μM – 10 μM of $\text{Cu}(\text{NO}_3)_2$ and 100 mM NaCl in 20 mM MOPS buffer (pH 6.5).

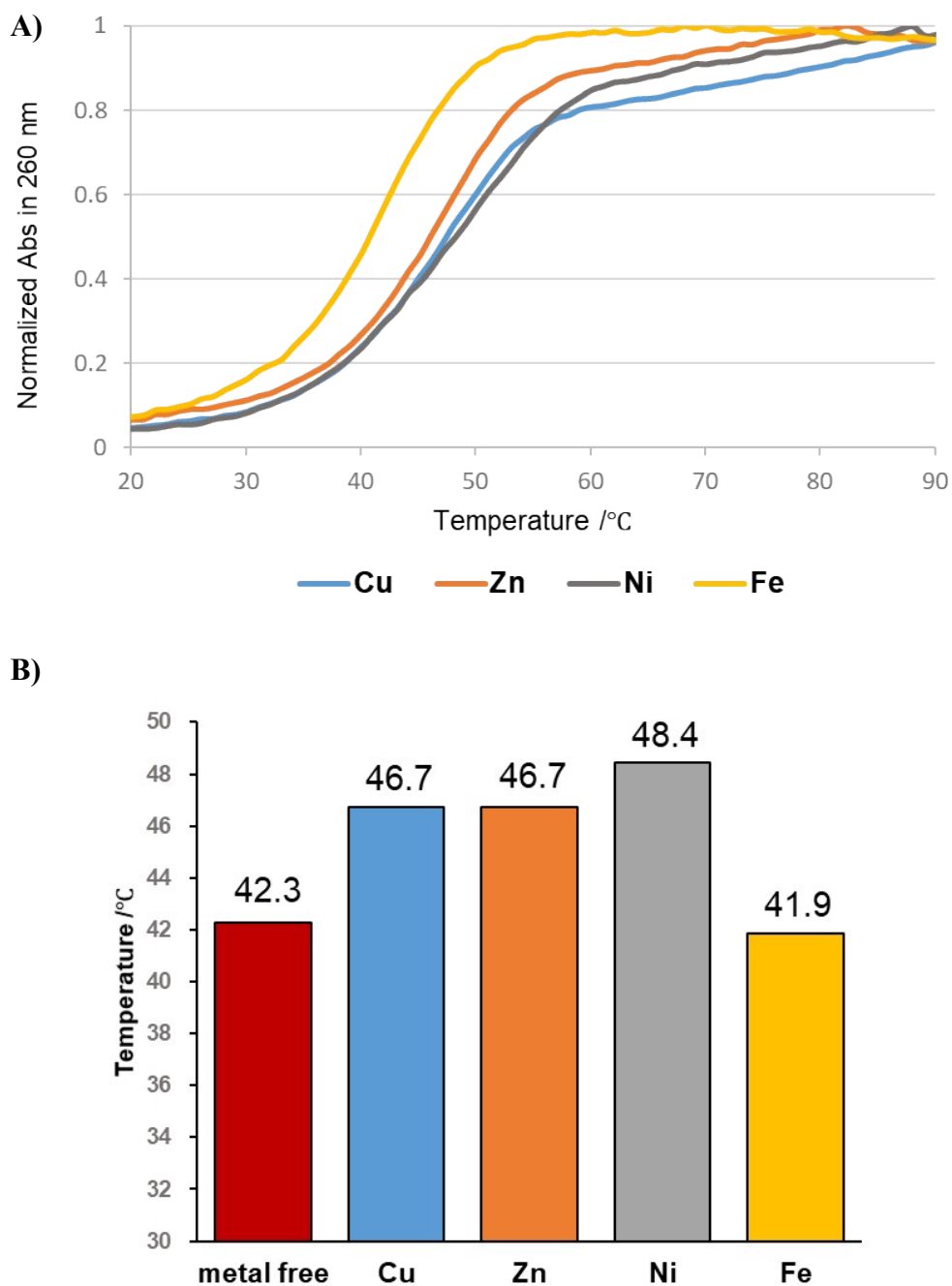


A) UV-melting curve of the duplexes ODN 14/ODN 15 with various equivalent of Cu^{2+} , B) T_m

value graph of the duplexes ODN 14/ODN 15 with various equivalent of Cu^{2+} .

Figure S8. Melting curves and T_m values of the duplexes ODN 1/ODN 2 (His) in the presence of 1 equivalent of metal ions ^a

^a Solution conditions: 2.5 μM each DNA, 2.5 μM of various metal ions and 100 mM NaCl in 20 mM MOPS buffer (pH 6.5).

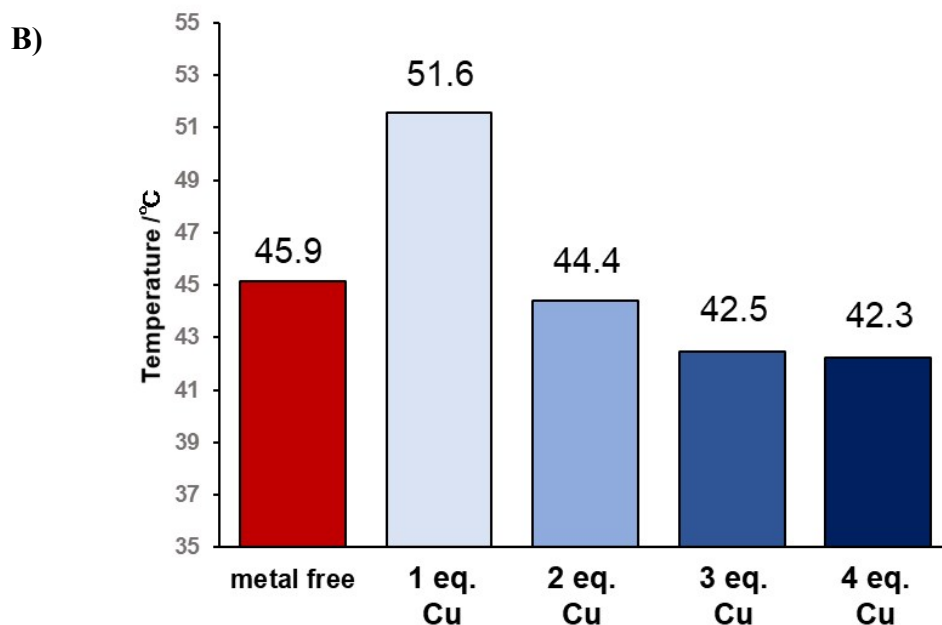
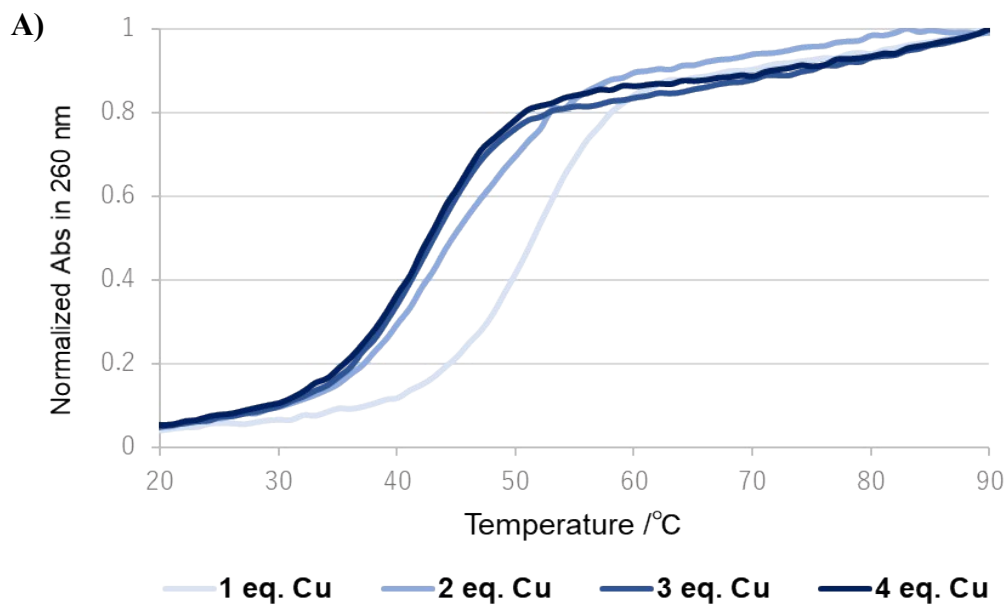


A) UV-melting curve of the duplexes ODN 1/ODN 2 (His) with 1 equivalent of metal ions, B) T_m

value graph of the duplexes ODN 1/ODN 2 (His) with 1 equivalent of metal ions.

Figure S9. Melting curves and T_m values of the duplexes ODN 1/ODN 2 (His) in the presence of 1-4 equivalent of Cu^{2+} ^a

^a Solution conditions: 2.5 μM each DNA, 2.5 μM – 10 μM of $\text{Cu}(\text{NO}_3)_2$ and 100 mM NaCl in 20 mM MOPS buffer (pH 6.5).

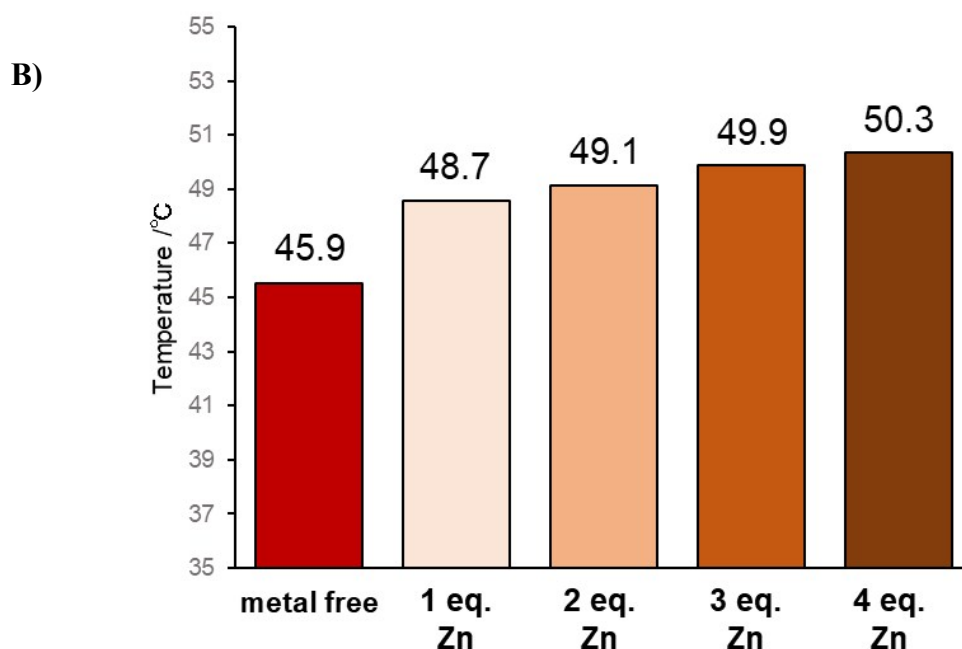
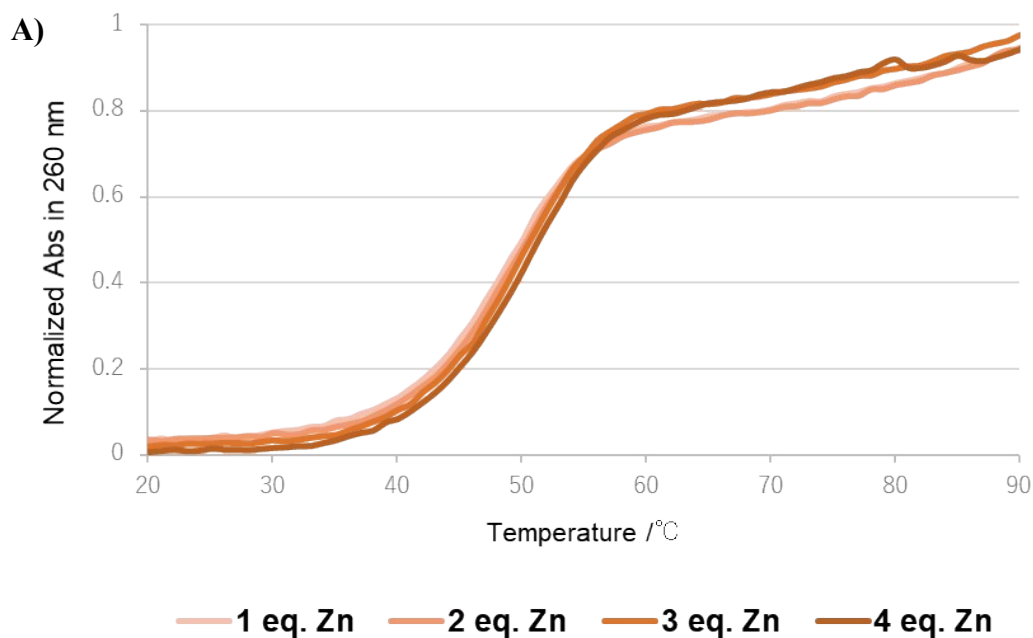


A) UV-melting curve of the duplexes **ODN 1/ODN 2 (His)** with various equivalent of Cu^{2+} , B) T_m

value graph of the duplexes **ODN 1/ODN 2 (His)** with various equivalent of Cu^{2+} .

Figure S10. Melting curves and T_m values of the duplexes ODN 1/ODN 2 (His) in the presence of 1-4 equivalent of Zn^{2+} ^a

^a Solution conditions: 2.5 μ M each DNA, 2.5 μ M – 10 μ M of $ZnCl_2$ and 100 mM NaCl in 20 mM MOPS buffer (pH 6.5).

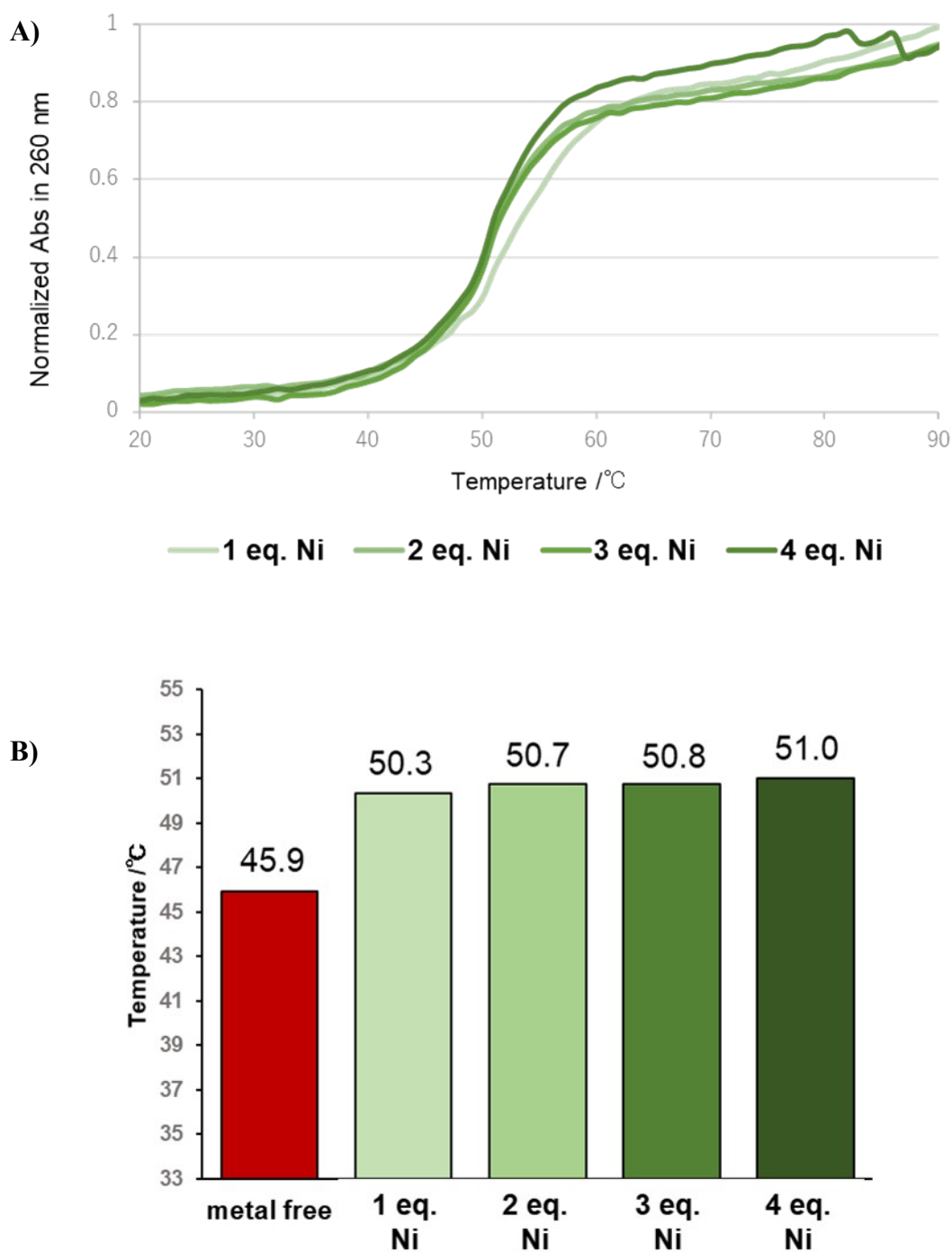


A) UV-melting curve of the duplexes **ODN 1/ODN 2 (His)** with various equivalent of Zn^{2+} , B) T_m

value graph of the duplexes **ODN 1/ODN 2 (His)** with various equivalent of Zn^{2+} .

Figure S11. Melting curves and T_m values of the duplexes ODN 1/ODN 2 (His) in the presence of 1-4 equivalent of Ni^{2+} ^a

^a Solution conditions: 2.5 μM each DNA, 2.5 μM – 10 μM of NiCl_2 and 100 mM NaCl in 20 mM MOPS buffer (pH 6.5).

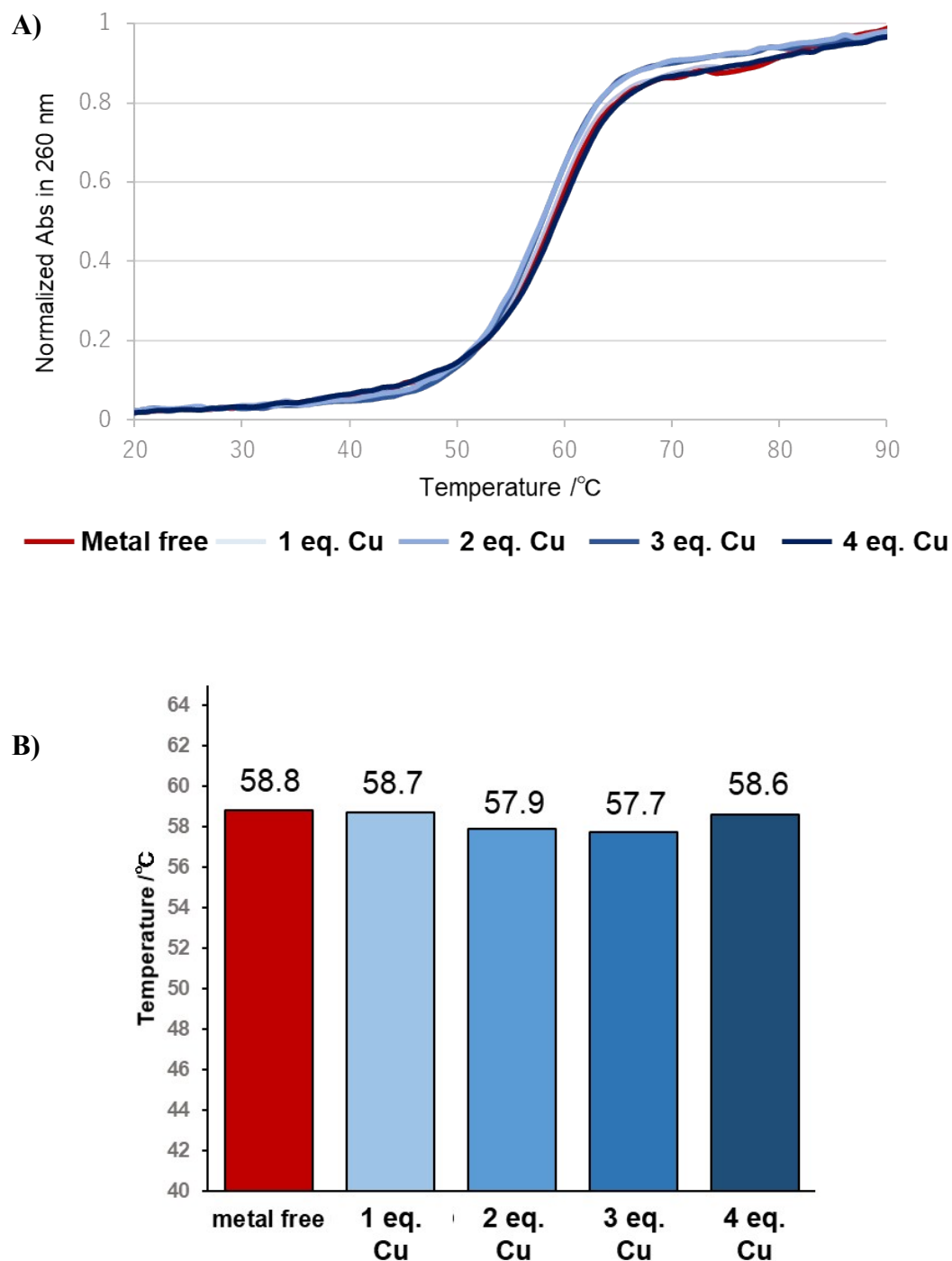


A) UV-melting curve of the duplexes ODN 1/ODN 2 (His) with various equivalent of Ni^{2+} , B) T_m

value graph of the duplexes ODN 1/ODN 2 (His) with various equivalent of Ni^{2+} .

Figure S12. Melting curves and T_m values of the duplexes ODN 16/ODN 17 in the presence of 1-4 equivalent of Cu^{2+}

^a Solution conditions: 2.5 μM each DNA, 2.5 μM – 10 μM of $\text{Cu}(\text{NO}_3)_2$ and 100 mM NaCl in 20 mM MOPS buffer (pH 6.5).

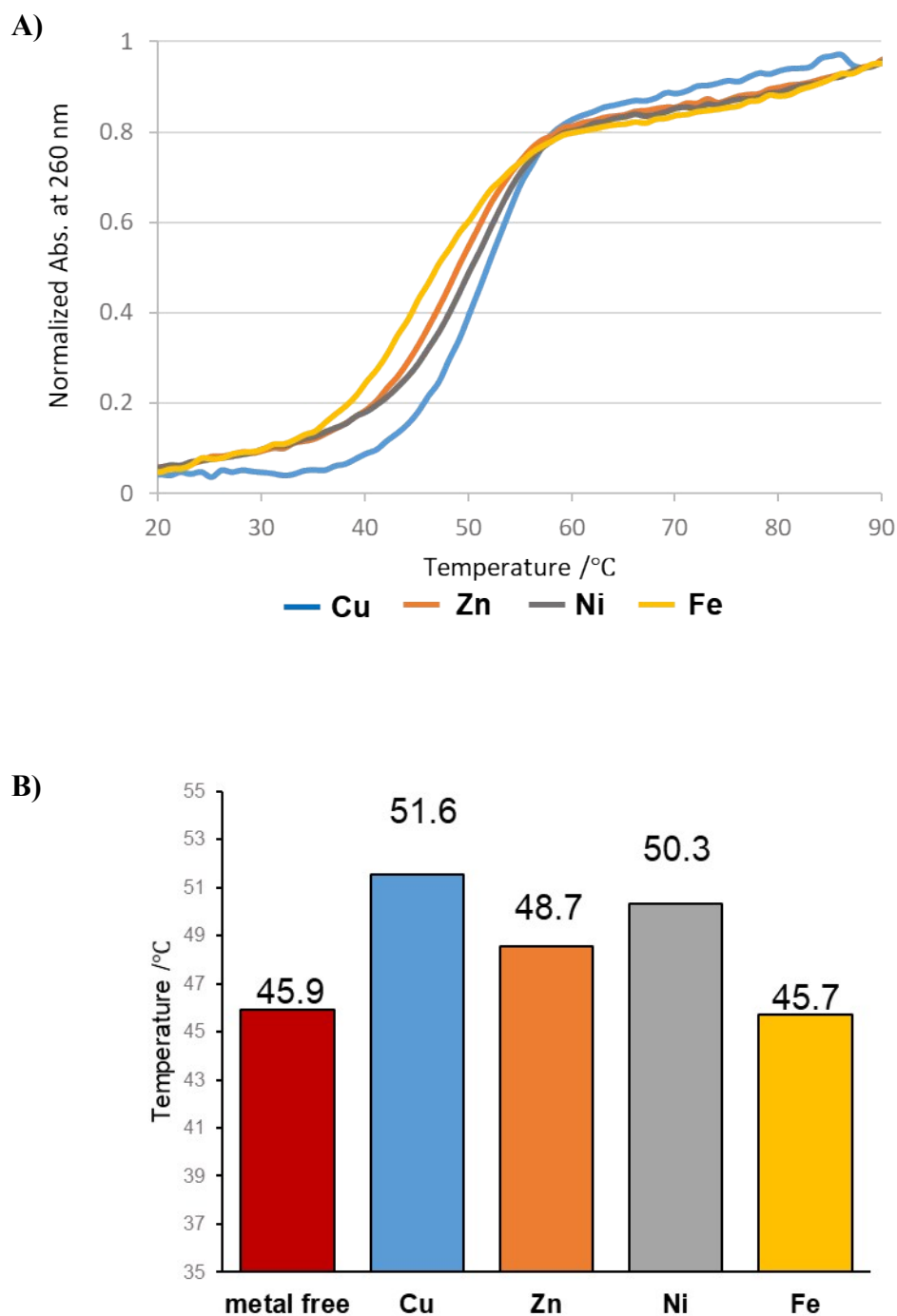


A) UV-melting curve of the duplexes ODN 16/ODN 17 with 1 equivalent of various metal ions,

B) T_m value graph of the duplexes ODN 16/ODN 17 with 1 equivalent of various metal ions.

Figure S13. Melting curves and T_m values of the duplexes ODN 5/ODN 6 in the presence of 1 equivalent of metal ions ^a

^a Solution conditions: 2.5 μ M each DNA, 2.5 μ M of various metal ions and 100 mM NaCl in 20 mM MOPS buffer (pH 6.5).

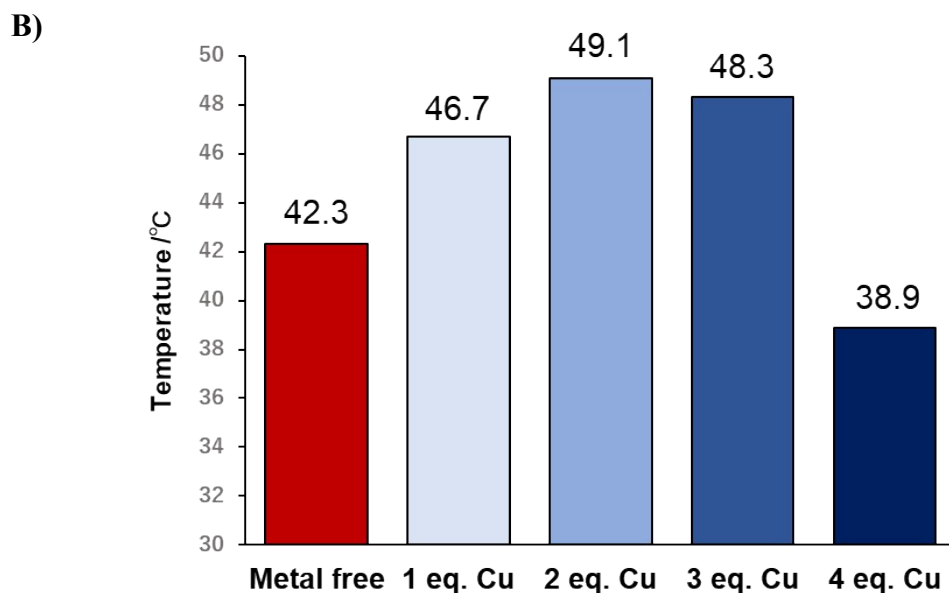
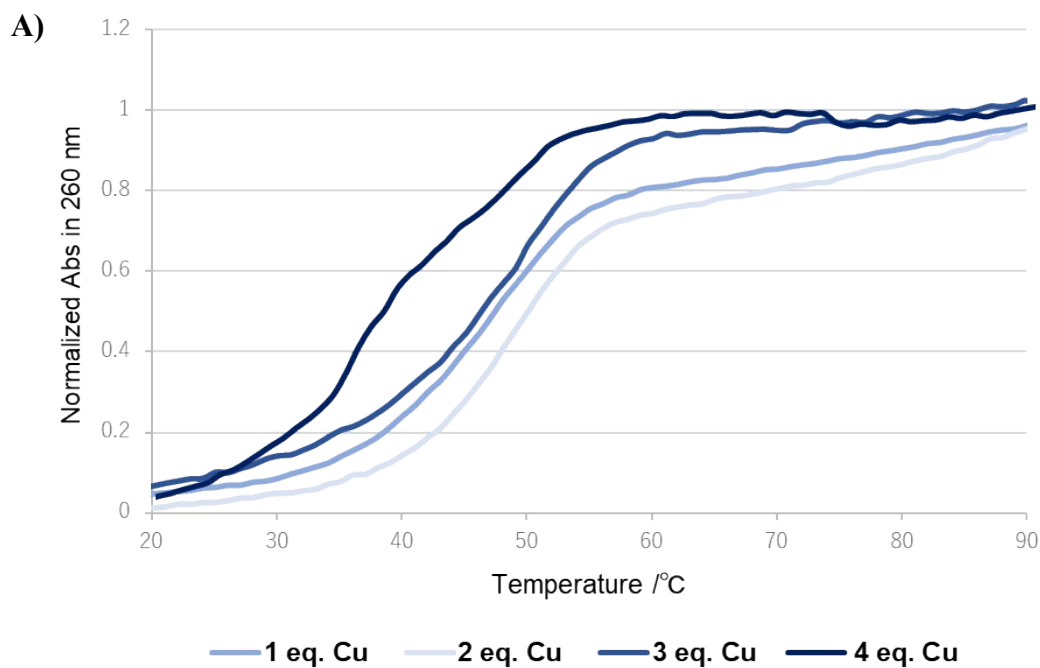


A) UV-melting curve of the duplexes ODN 5/ODN 6 with 1 equivalent of various metal ions, B)

T_m value graph of the duplexes ODN 5/ODN 6 with 1 equivalent of various metal ions.

Figure S14. Melting curves and T_m values of the duplexes ODN 5/ODN 6 in the presence of 1-4 equivalent of Cu^{2+}

^a Solution conditions: 2.5 μM each DNA, 2.5 μM – 10 μM of $\text{Cu}(\text{NO}_3)_2$ and 100 mM NaCl in 20 mM MOPS buffer (pH 6.5).

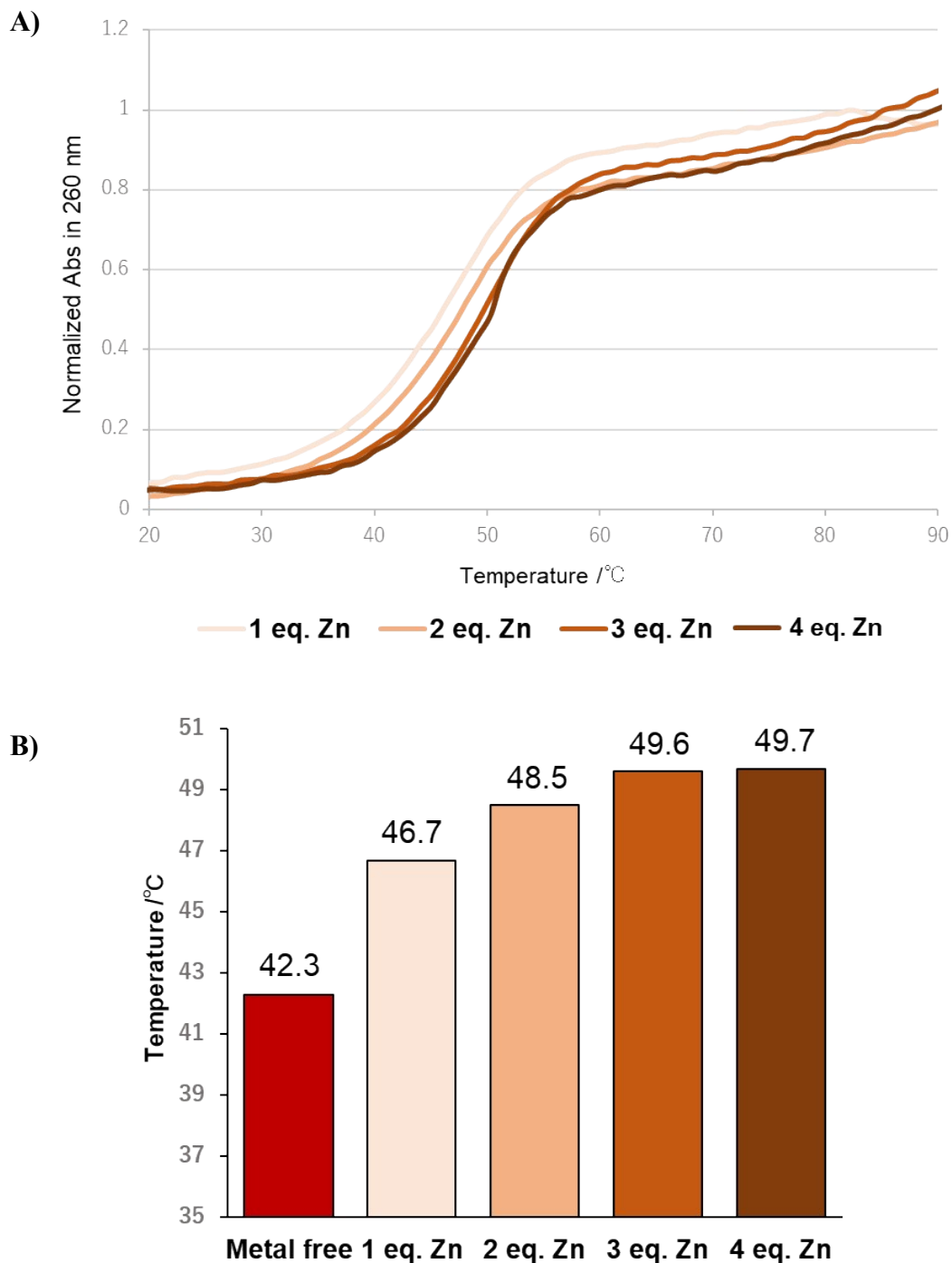


A) UV-melting curve of the duplexes ODN 5/ODN 6 with various equivalent of Cu^{2+} , B) T_m value

graph of the duplexes ODN 5/ODN 6 with various equivalent of Cu^{2+} .

Figure S15. Melting curves and T_m values of the duplexes ODN 5/ODN 6 in the presence of 1-4 equivalent of Zn^{2+} ^a

^a Solution conditions: 2.5 μ M each DNA, 2.5 μ M – 10 μ M of $ZnCl_2$ and 100 mM NaCl in 20 mM MOPS buffer (pH 6.5).

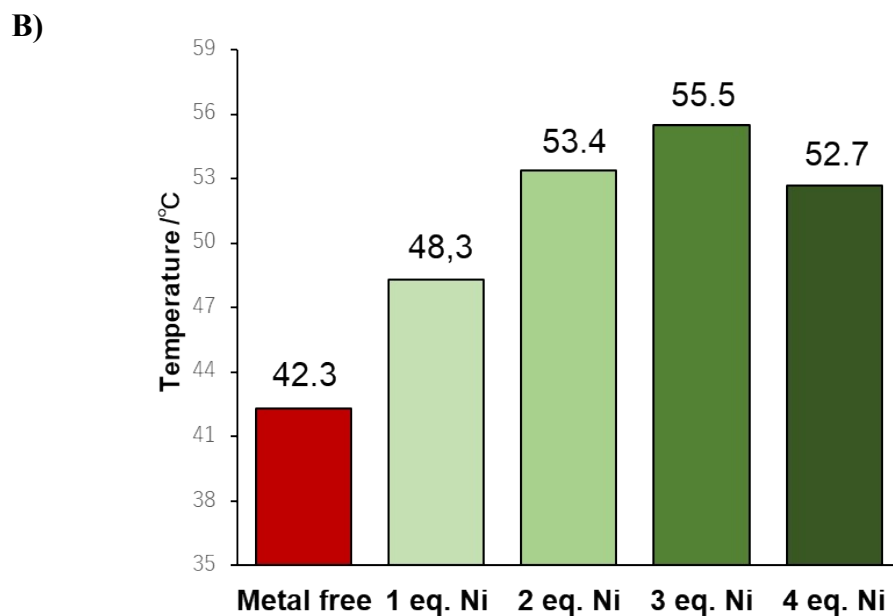
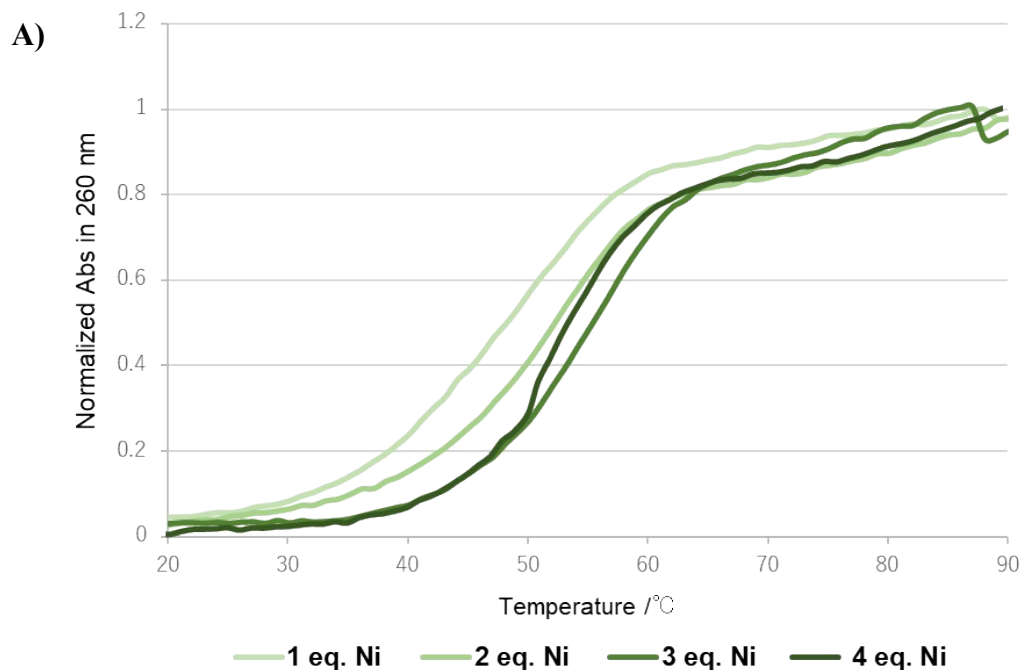


A) UV-melting curve of the duplexes ODN 5/ODN 6 with various equivalent of Zn^{2+} , B) T_m value

graph of the duplexes ODN 5/ODN 6 with various equivalent of Zn^{2+} .

Figure S16. Melting curves and T_m values of the duplexes ODN 5/ODN 6 in the presence of 1-4 equivalent of Ni^{2+}

^a Solution conditions: 2.5 μM each DNA, 2.5 μM – 10 μM of NiCl_2 and 100 mM NaCl in 20 mM MOPS buffer (pH 6.5).

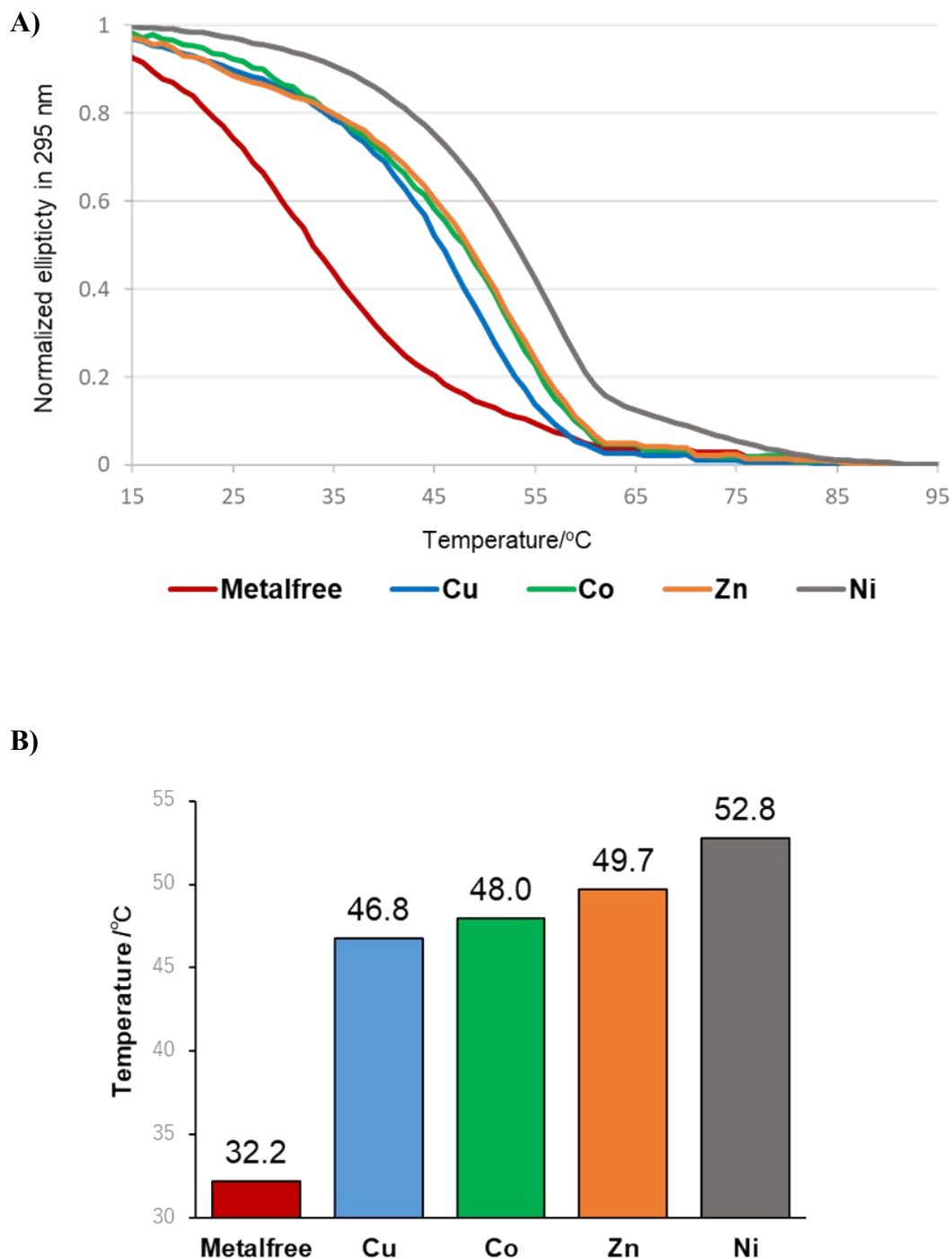


A) UV-melting curve of the duplexes **ODN 5/ODN 6** with various equivalent of Ni^{2+} , B) T_m value

graph of the duplexes **ODN 5/ODN 6** with various equivalent of Ni^{2+} .

Figure S17. Melting curves and T_m values of DNA quadruplex-duplex hybrids ODN 10/ODN 11 in the presence of 1 equivalent of various metal ions^a

^a Solution conditions: 7 μ M each DNA, 6.7 μ M of various metal ions and 100 mM KCl in 20 mM Tris-HCl buffer (pH 7.4).

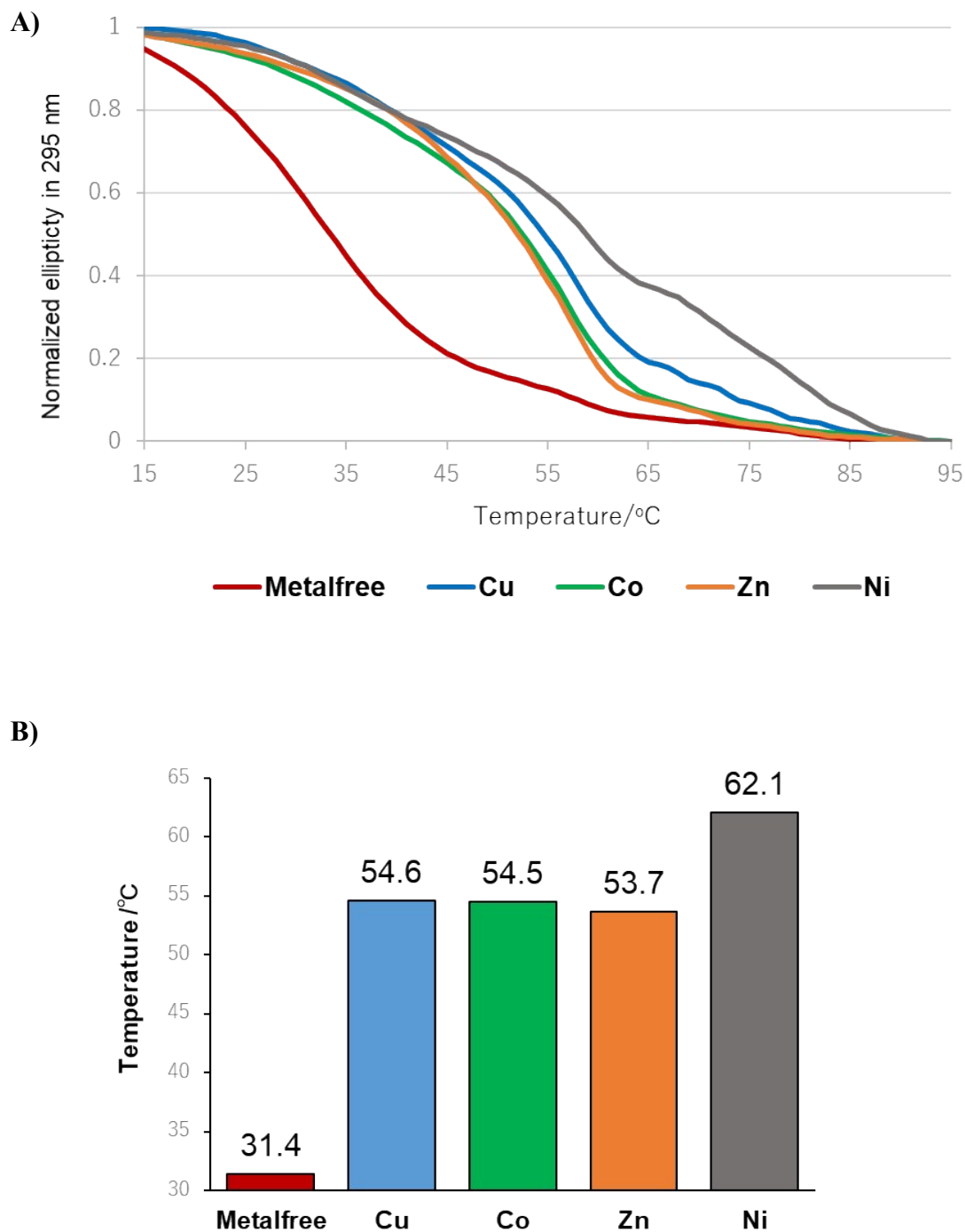


A) UV-melting curve of quadruplex-duplex ODN 10/ODN 11 with various metal ions, B) T_m

value graph of quadruplex-duplex ODN 10/ODN 11 with various metal ions.

Figure S18. Melting curves and T_m values of DNA quadruplex-duplex hybrids ODN 12/ODN 13 in the presence of 1 equivalent of various metal ions^a

^a Solution conditions: 7 μM each DNA, 6.7 μM of various metal ions and 100 mM KCl in 20 mM Tris-HCl buffer (pH 7.4).

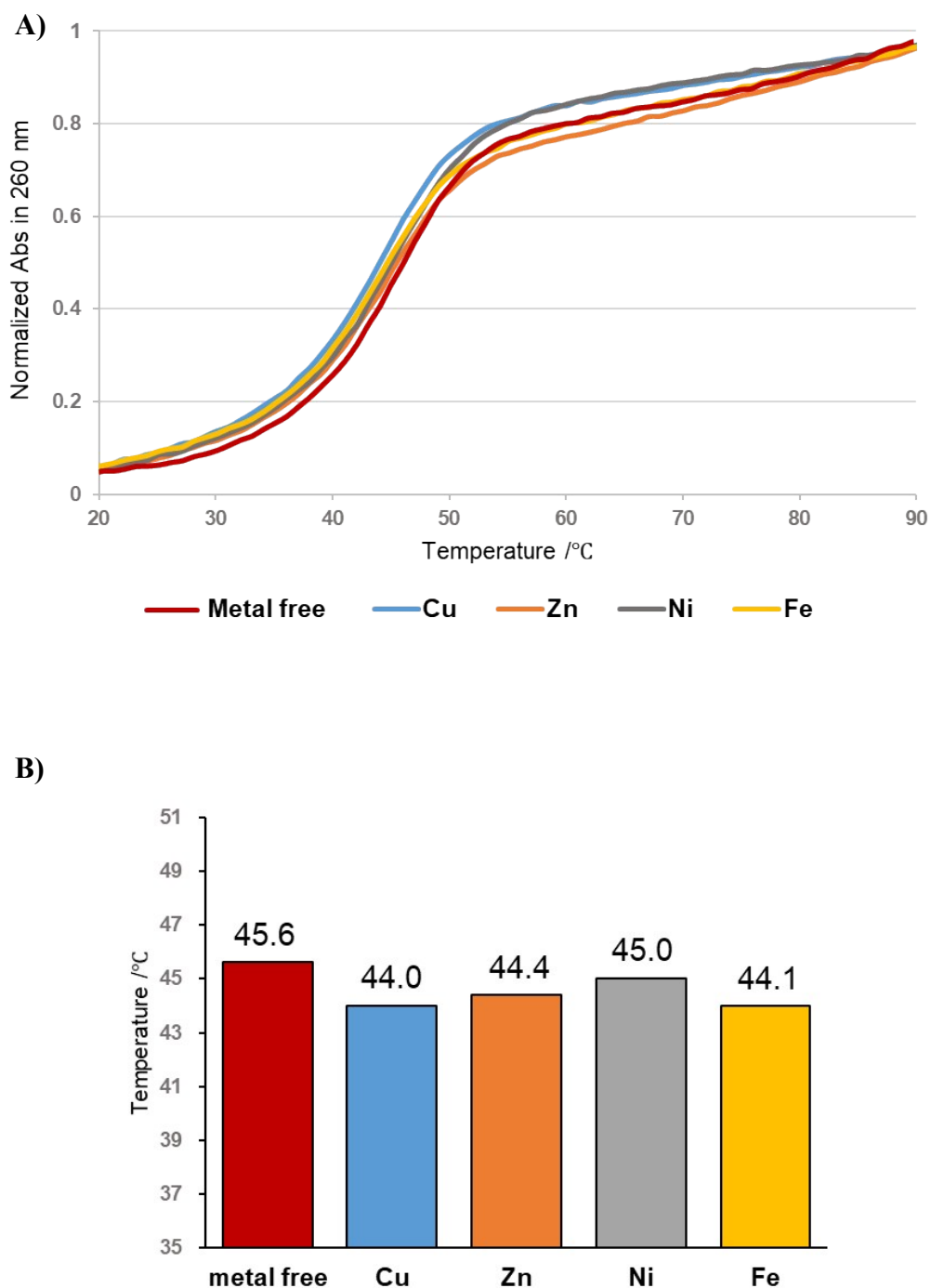


A) UV-melting curve of quadruplex-duplex ODN 12/ODN 13 with various metal ions, B) T_m

value graph of quadruplex-duplex ODN 12/ODN 13 with various metal ions.

Figure S19. Melting curves and T_m values of the duplex ODN 20/ODN 21 in the presence of 1 equivalent of various metal ions ^a

^a Solution conditions: 2.5 μ M each DNA, 2.5 μ M of various metal ions and 100 mM NaCl in 20 mM MOPS buffer (pH 6.5).

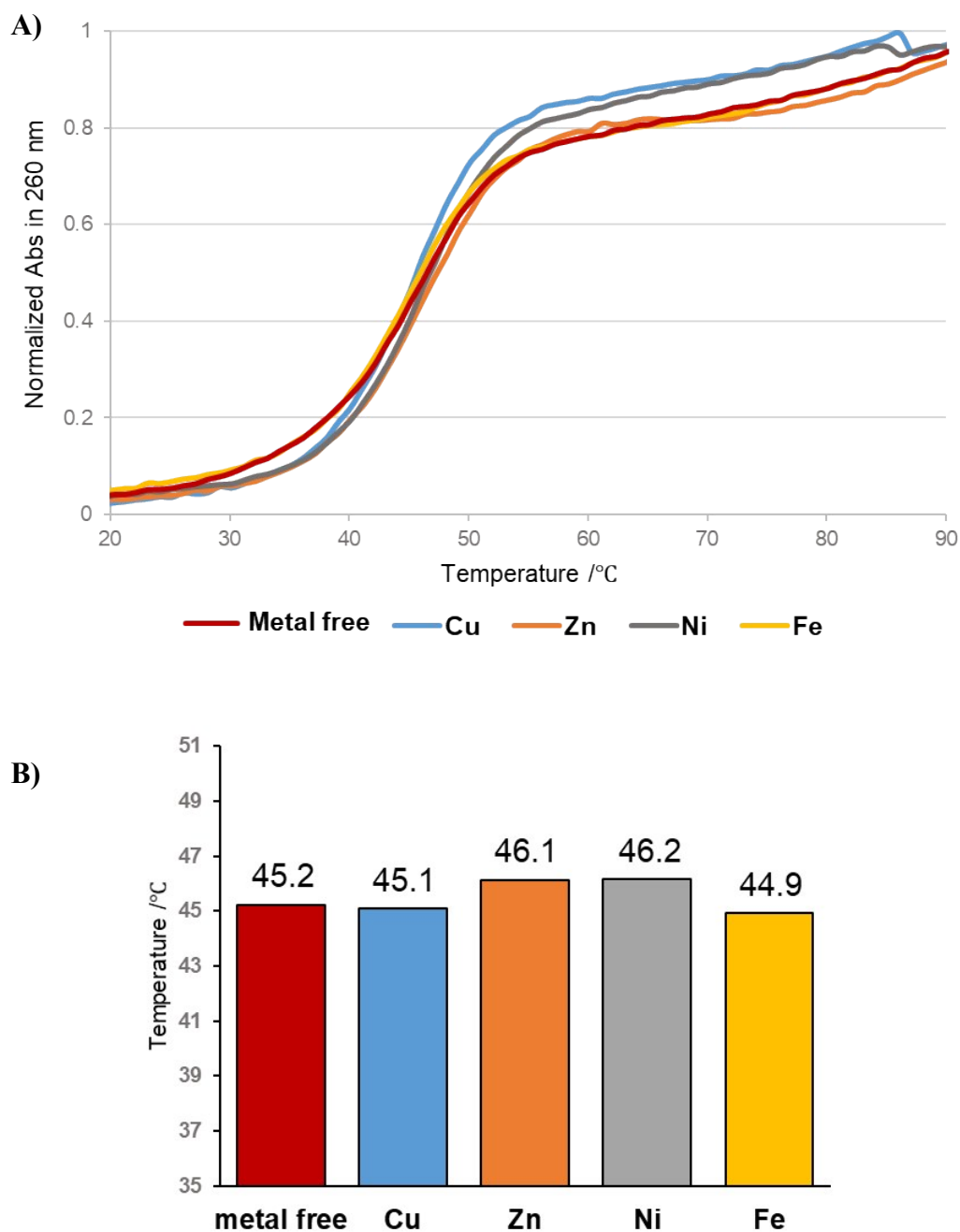


A) UV-melting curve of quadruplex-duplex ODN 20/ODN 21 with various metal ions, B) T_m

value graph of quadruplex-duplex ODN 20/ODN 21 with various metal ions.

Figure S20. Melting curves and T_m values of the duplex ODN 22/ODN 23 in the presence of 1 equivalent of various metal ions ^a

^a Solution conditions: 2.5 μ M each DNA, 2.5 μ M of various metal ions and 100 mM NaCl in 20 mM MOPS buffer (pH 6.5).



A) UV-melting curve of quadruplex-duplex ODN 22/ODN 23 with various metal ions, B) T_m

value graph of quadruplex-duplex ODN 22/ODN 23 with various metal ions.

CD Spectroscopy

CD spectra of oligonucleotide solutions collected in 0.5-nm steps from 320 to 220 nm were measured using JASCO J-805LST Spectrometer in a 1-cm quartz cuvette. Each spectrum shown is the average of two individual scans. The samples were denatured at 95 °C for 4 min and annealed slowly to RT then stored at 5 °C until experiments were initiated. All samples were prepared in a total volume of 150 µl containing 6.0 µM of each duplex forming oligonucleotides, 6.0 µM Cu(NO₃)₂, (ZnCl₂, NiCl₂, and FeCl₃), 20 mM MOPS buffer (pH 6.5) and 100 mM NaCl. Or 7.0 µM of each quadruplex-duplex forming oligonucleotides, 6.7 µM Cu(NO₃)₂, (ZnCl₂, NiCl₂, CoCl₂, and FeCl₃), 20 mM Tris-HCl buffer (pH 7.4) and 100 mM KCl.

Figure S21. CD spectra of the duplexes ODN 1/ODN 2 (Y) in the presence of 1 equivalent of metal ions ^a

^a Solution conditions: 6.0 μM each DNA, 6.0 μM of various metal ions and 100 mM NaCl in 20 mM MOPS buffer (pH 6.5).

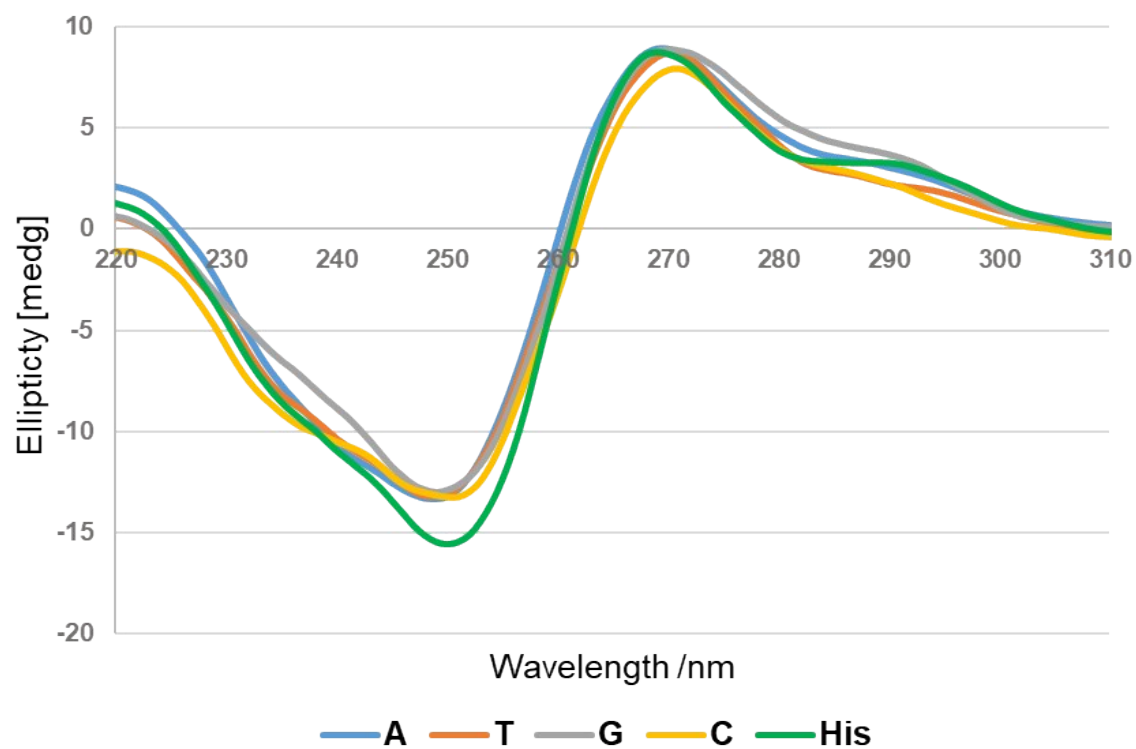


Figure S22. CD spectra of the duplexes ODN 3/ODN 4 (Y) in the presence of 1 equivalent of metal ions^a

^a Solution conditions: 6.0 μM each DNA, 6.0 μM of various metal ions and 100 mM NaCl in 20 mM MOPS buffer (pH 6.5).

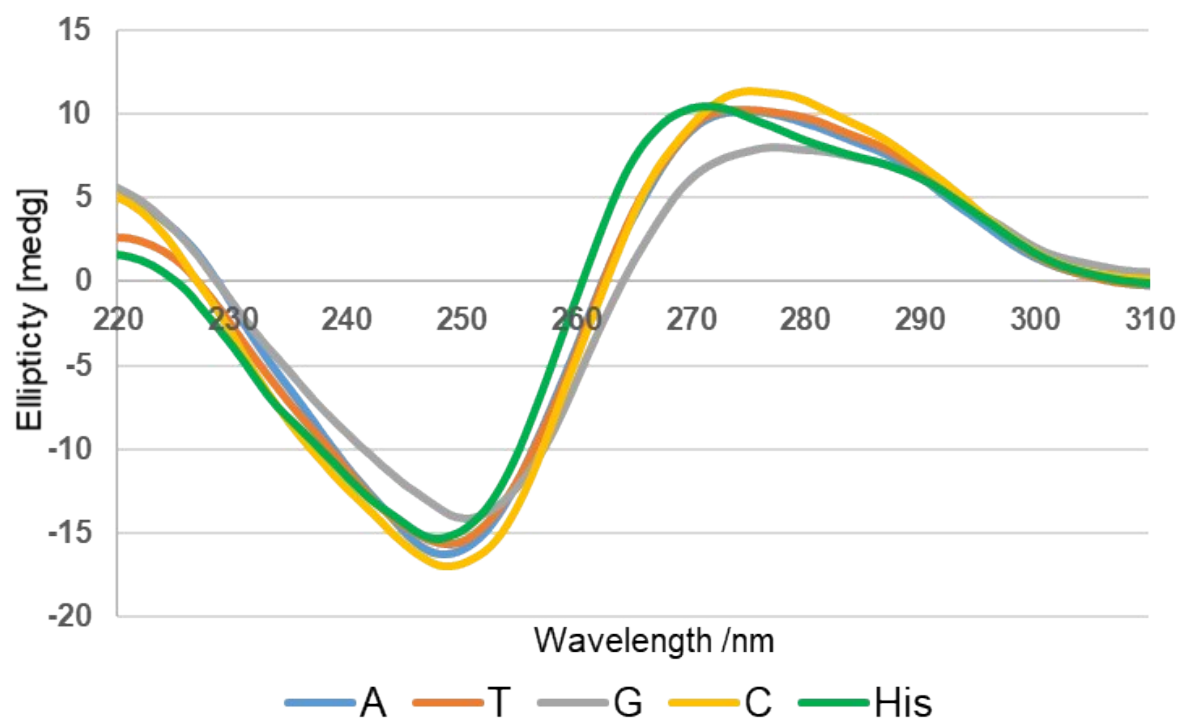


Figure S23. CD spectra of the duplexes ODN 1/ODN 2 (His) in the presence of 1 equivalent of metal ions ^a

^a Solution conditions: 6.0 μ M each DNA, 6.0 μ M of various metal ions and 100 mM NaCl in 20 mM MOPS buffer (pH 6.5).

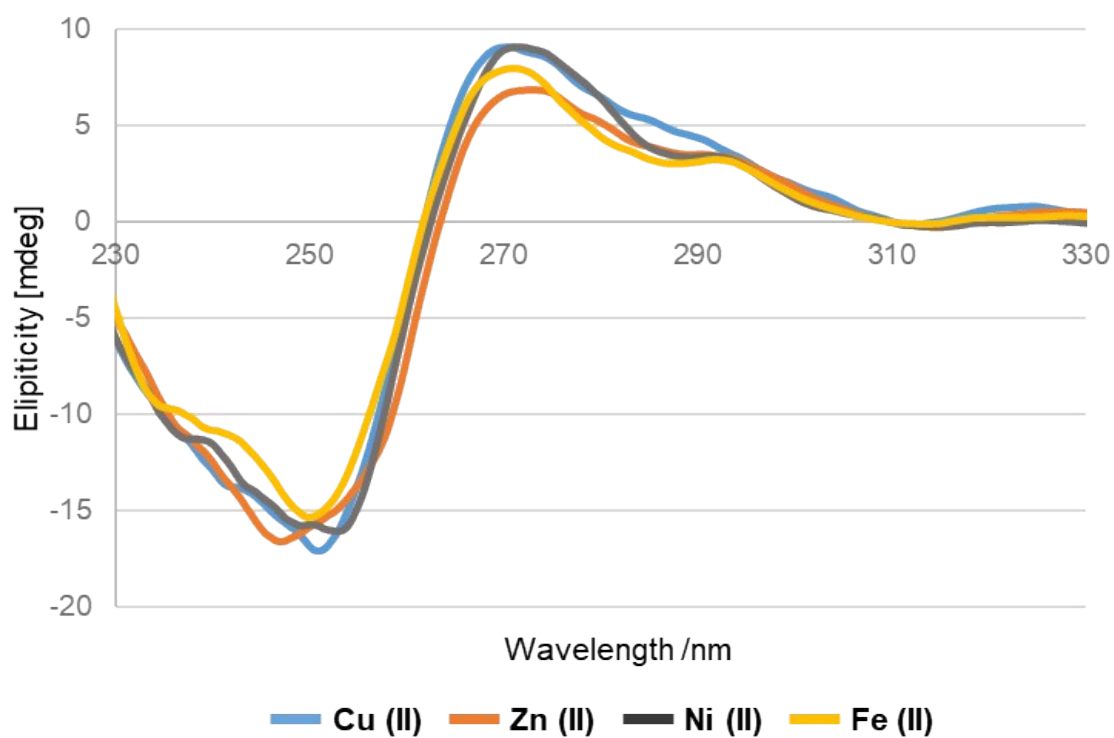


Figure S24. CD spectra of the duplexes ODN 1/ODN 2 (His) in the presence of 1-4 equivalent of Cu^{2+} ^a

^a Solution conditions: 6.0 μM each DNA, 6.0 μM – 24 μM of $\text{Cu}(\text{NO}_3)_2$ and 100 mM NaCl in 20 mM MOPS buffer (pH 6.5).

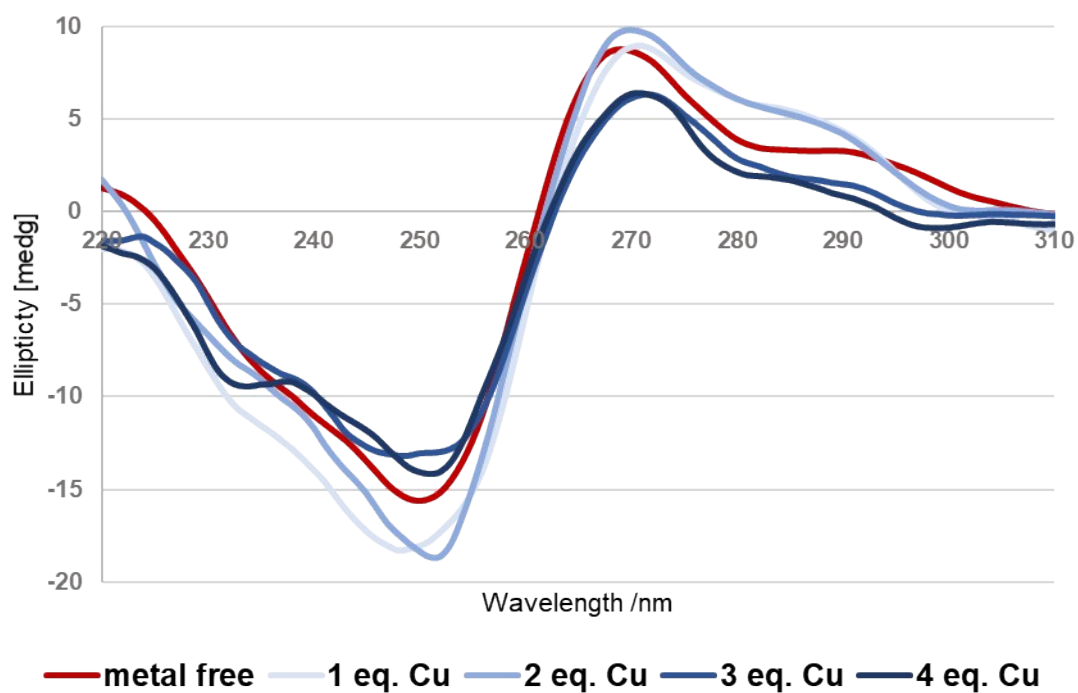


Figure S25. CD spectra of the duplexes ODN 1/ODN 2 (His) in the presence of 1-4 equivalent of Zn²⁺ ^a

^a Solution conditions: 6.0 μM each DNA, 6.0 μM – 24 μM of ZnCl₂ and 100 mM NaCl in 20 mM MOPS buffer (pH 6.5).

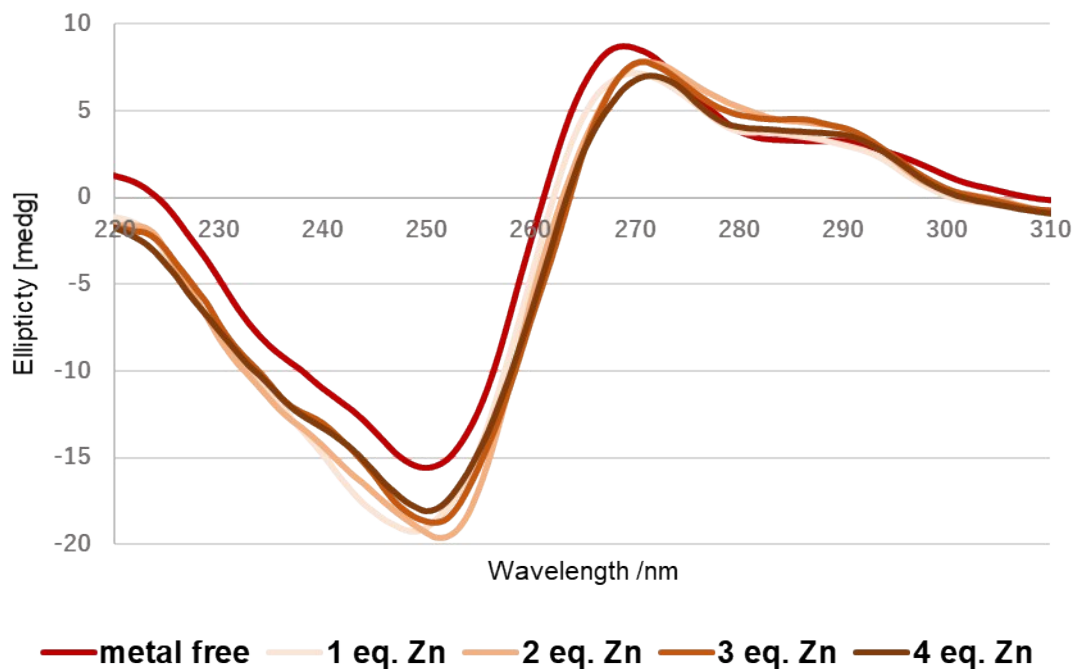


Figure S26. CD spectra of the duplexes ODN 1/ODN 2 (His) in the presence of 1-4 equivalent of Ni²⁺ ^a

^a Solution conditions: 6.0 μ M each DNA, 6.0 μ M – 24 μ M of NiCl₂ and 100 mM NaCl in 20 mM MOPS buffer (pH 6.5).

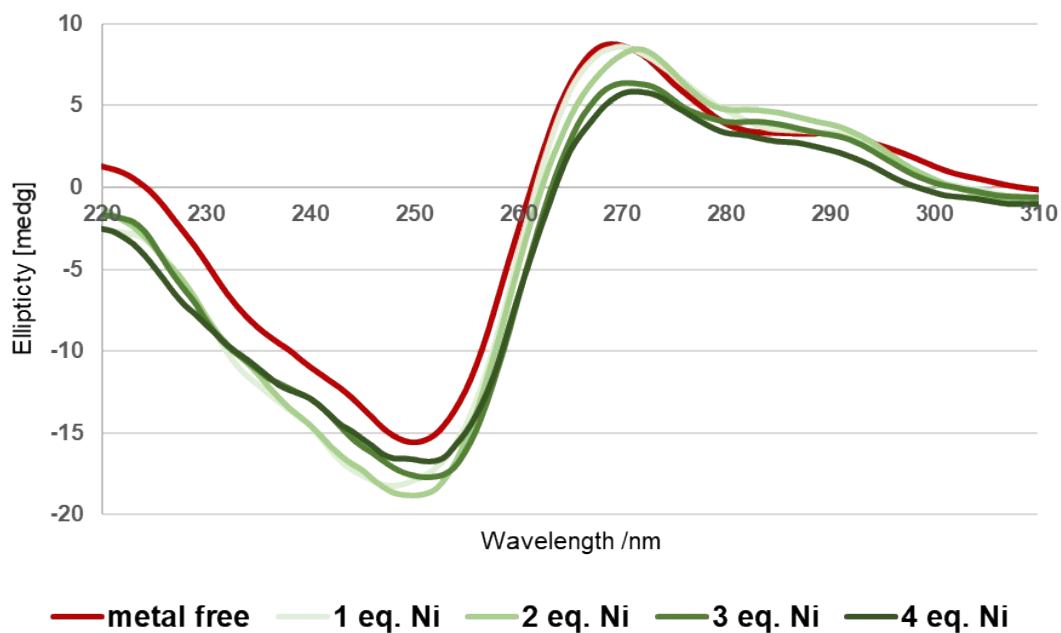


Figure S27. CD spectra of the duplexes ODN 16/ODN 17 in the presence of 1-4 equivalent of Cu^{2+} ^a

^a Solution conditions: 6.0 μM each DNA, 6.0 μM – 24 μM of $\text{Cu}(\text{NO}_3)_2$ and 100 mM NaCl in 20 mM MOPS buffer (pH 6.5).

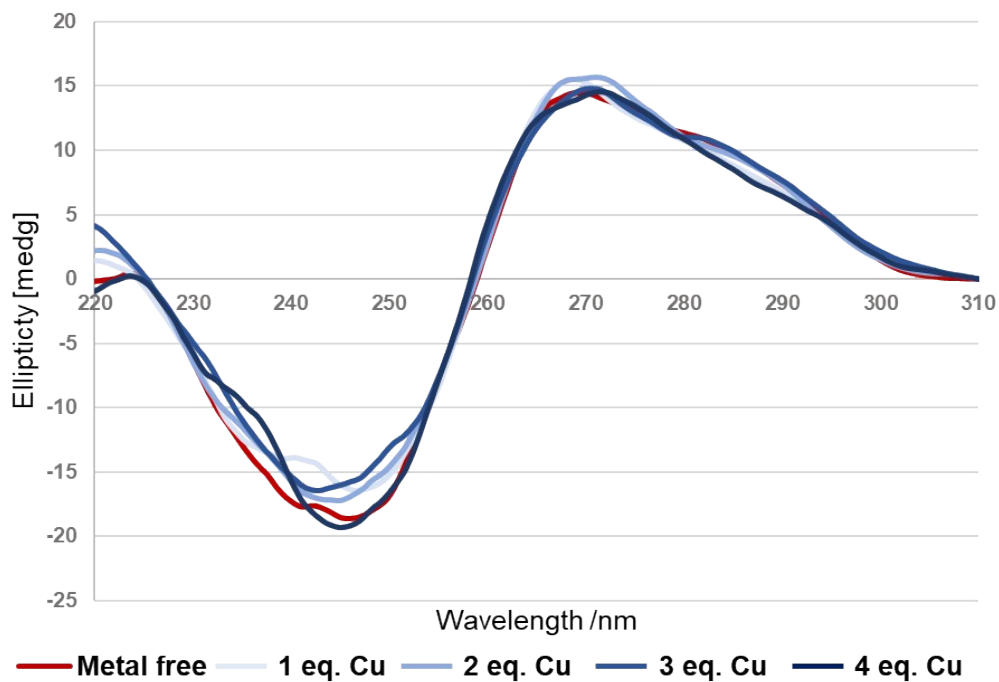


Figure S28. CD spectra of the duplexes ODN 5/ODN 6 in the presence of 1 equivalent of metal ions ^a

^a Solution conditions: 6.0 μM each DNA, 6.0 μM of various metal ions and 100 mM NaCl in 20 mM MOPS buffer (pH 6.5).

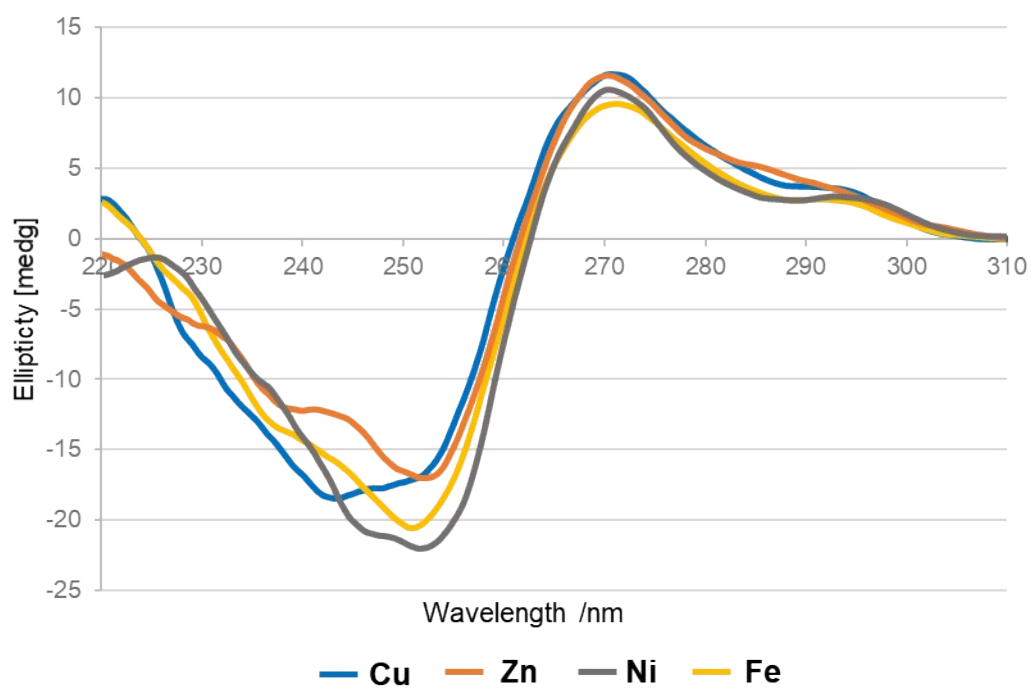


Figure S29. CD spectra of the duplexes ODN 5/ODN 6 in the presence of 1-4 equivalent of Cu^{2+} ^a

^a Solution conditions: 6.0 μM each DNA, 6.0 μM – 24 μM of $\text{Cu}(\text{NO}_3)_2$ and 100 mM NaCl in 20 mM MOPS buffer (pH 6.5).

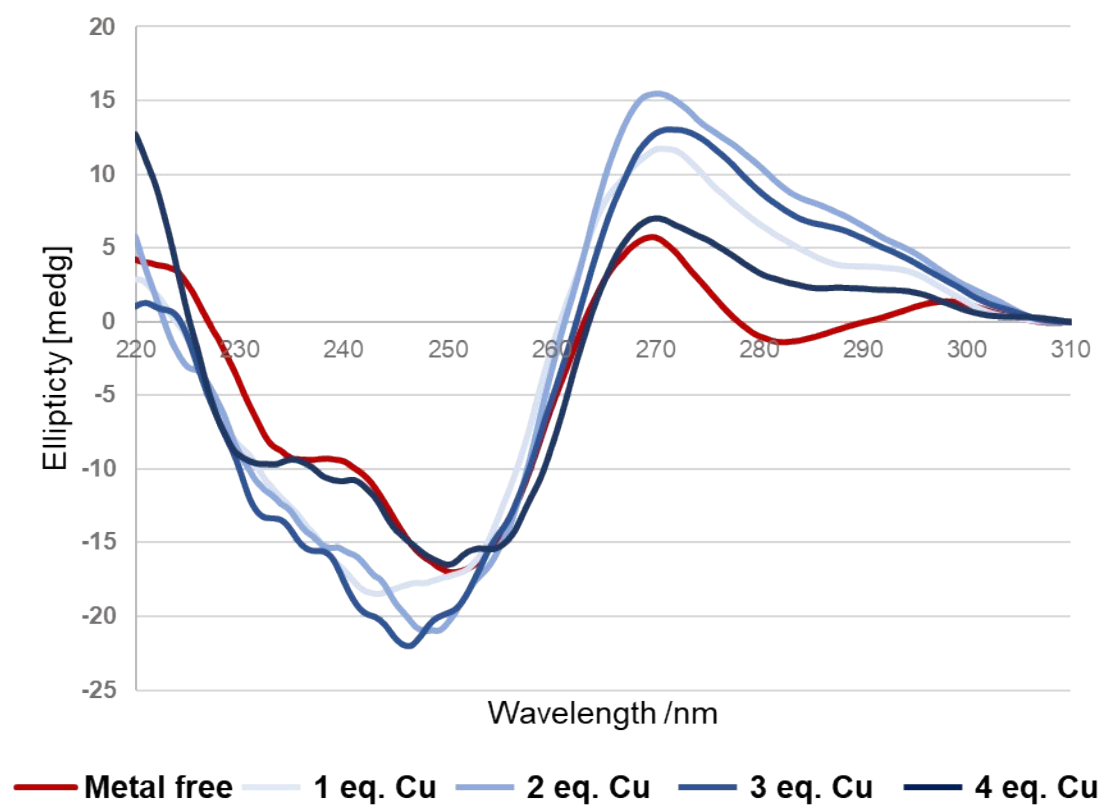


Figure S30. CD spectra of the duplexes ODN 5/ODN 6 in the presence of 1-4 equivalent of Zn^{2+} ^a

^a Solution conditions: 6.0 μ M each DNA, 6.0 μ M – 24 μ M of $ZnCl_2$ and 100 mM NaCl in 20 mM MOPS buffer (pH 6.5).

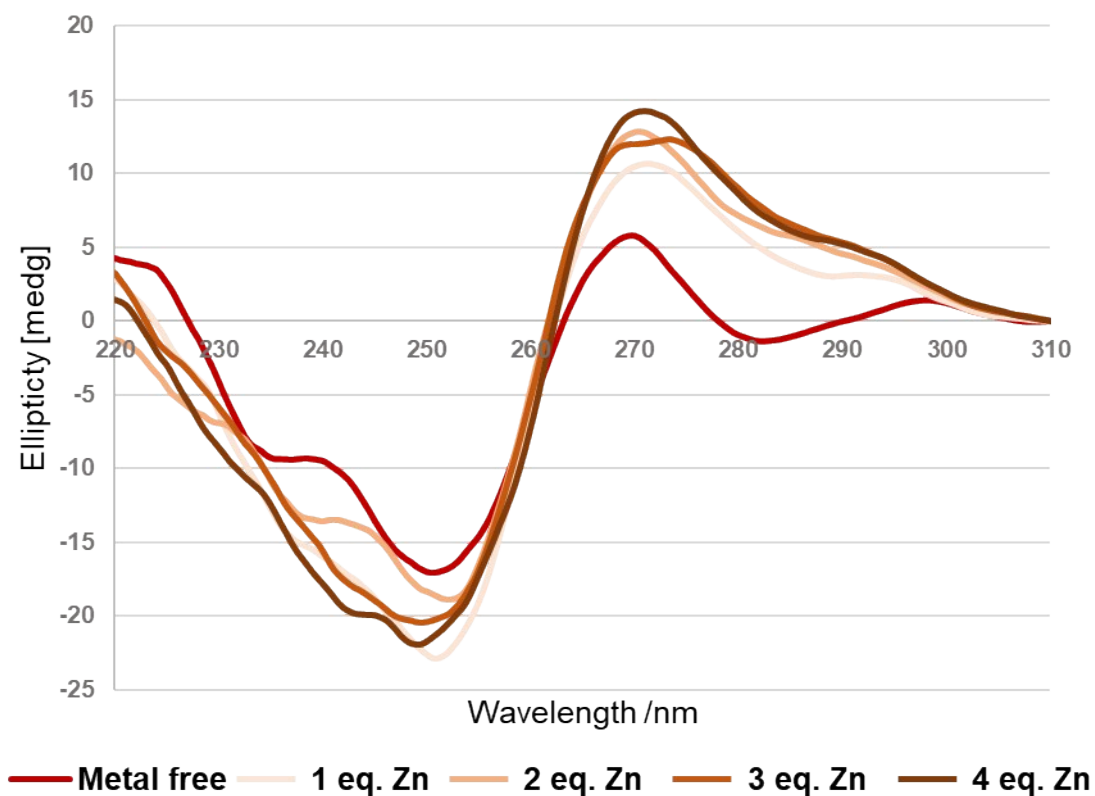


Figure S31. CD spectra of the duplexes ODN 5/ODN 6 in the presence of 1-4 equivalent of Ni²⁺ ^a

^a Solution conditions: 2.5 μ M each DNA, 2.5 μ M – 10 μ M of NiCl₂ and 100 mM NaCl in 20 mM MOPS buffer (pH 6.5).

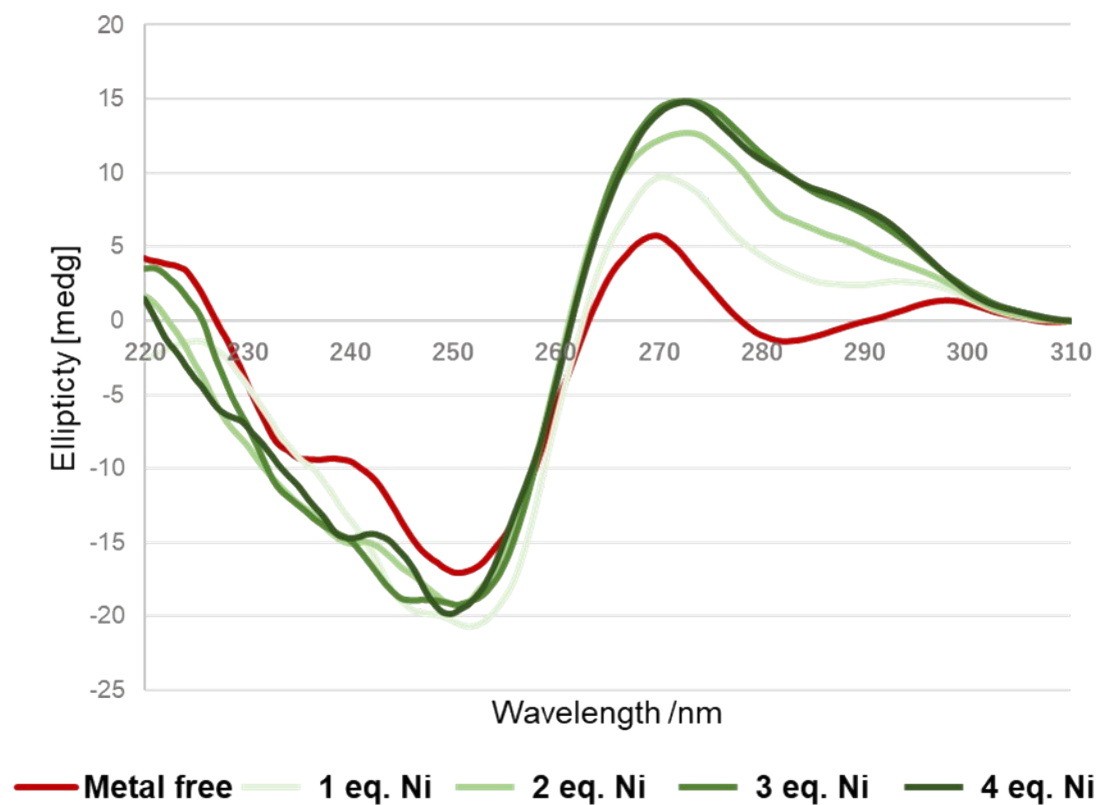


Figure S32. CD spectra of DNA quadruplex-duplex hybrids ODN 10/ODN 11 in the presence of 1 equivalent of various metal ions ^a

^a Solution conditions: 7 μ M each DNA, 6.7 μ M of various metal ions and 100 mM KCl in 20 mM Tris-HCl buffer (pH 7.4).

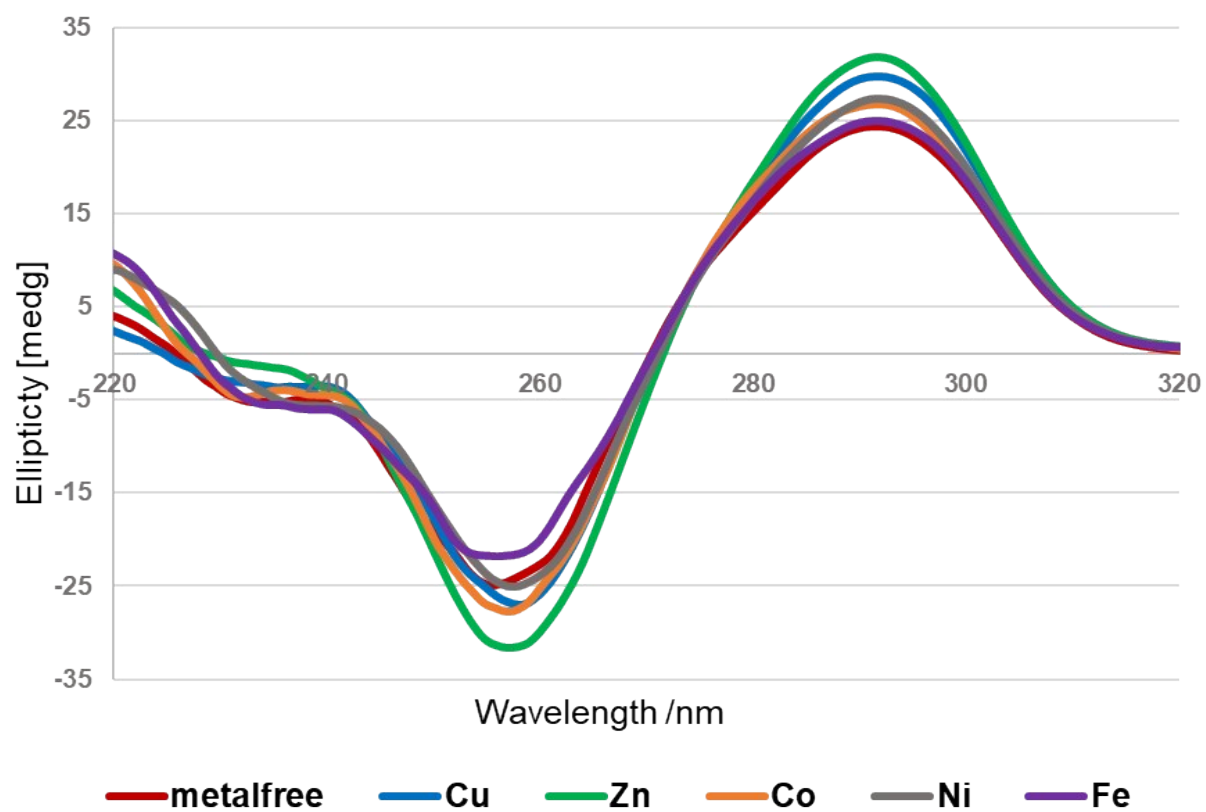


Figure S33. CD spectra of DNA quadruplex-duplex hybrids ODN 12/ODN 13 in the presence of 1 equivalent of various metal ions ^a

^a Solution conditions: 7 μM each DNA, 6.7 μM of various metal ions and 100 mM KCl in 20 mM Tris-HCl buffer (pH 7.4).

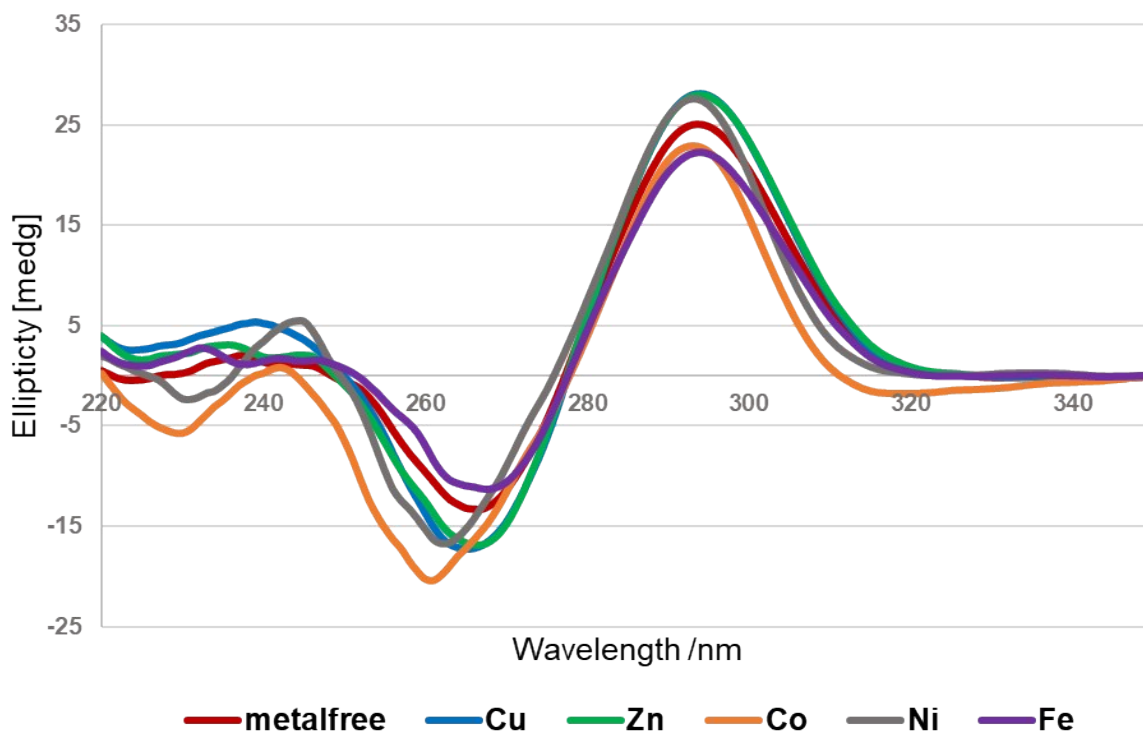


Figure S34. CD spectra of the duplex ODN 20/ODN 21 in the presence of 1 equivalent of various metal ions ^a

^a Solution conditions: 2.5 μ M each DNA, 2.5 μ M of various metal ions and 100 mM NaCl in 20 mM MOPS buffer (pH 6.5).

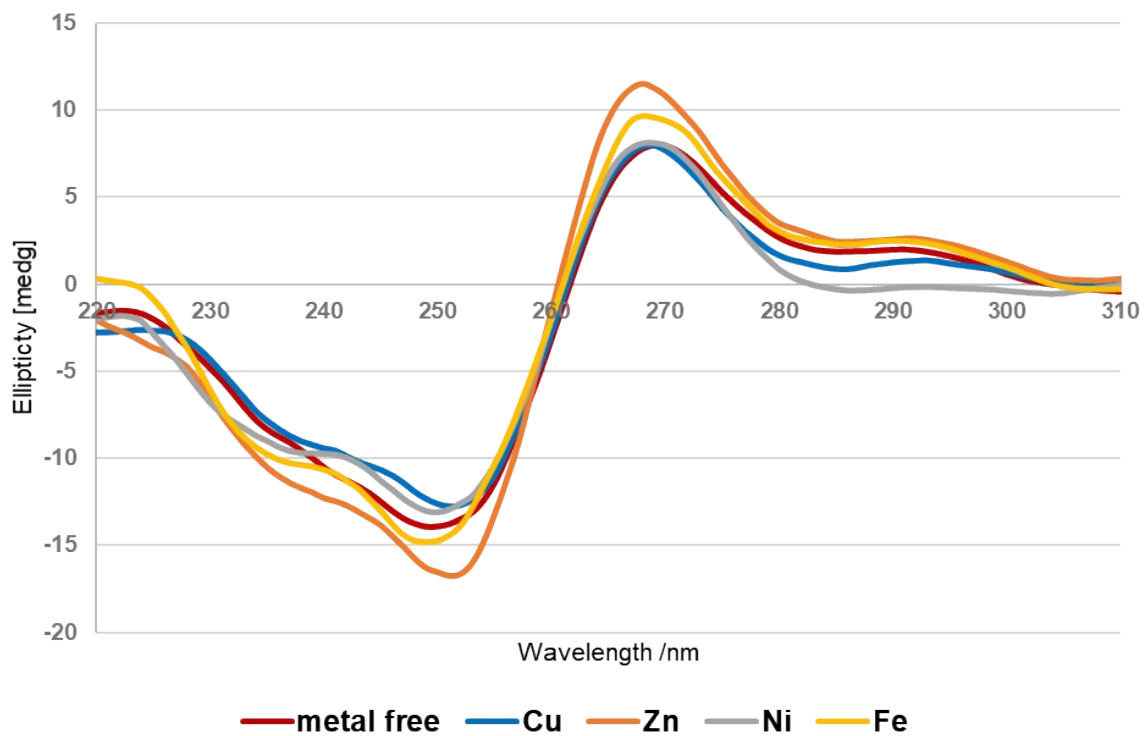
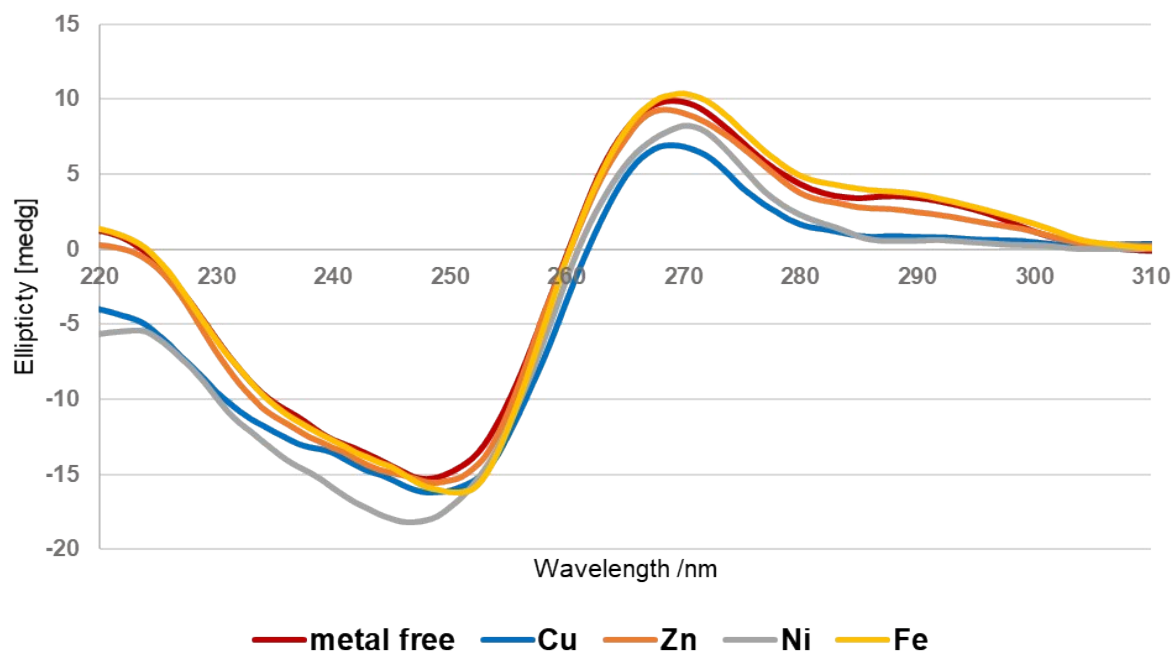


Figure S35. CD spectra of the duplex ODN 22/ODN 23 in the presence of 1 equivalent of various metal ions ^a

^a Solution conditions: 2.5 μ M each DNA, 2.5 μ M of various metal ions and 100 mM NaCl in 20 mM MOPS buffer (pH 6.5).

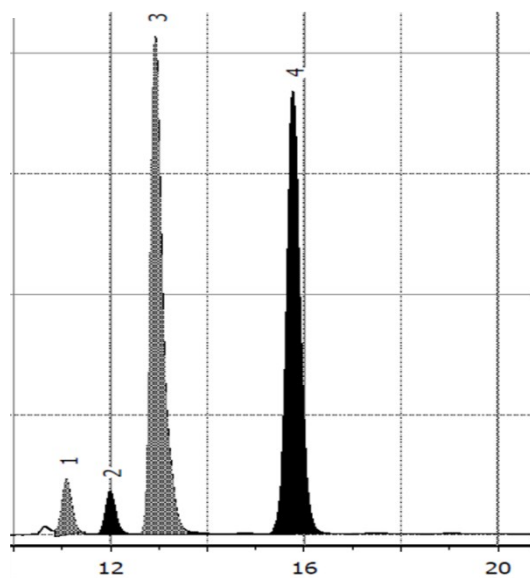


Asymmetric Diels-Alder Reactions Catalyzed by DNA-based Hybrid Catalysts

The DNA-based hybrid catalyst was prepared in solution by mixing the copper complex and DNA duplex. 40 nmol of the modified oligonucleotide with intrastrand ether linker or intrastrand alkyl linker and the equivalent complementary strand were mixed and freeze dried. Subsequently, 15 μL of 2 mM $\text{Cu}(\text{NO}_3)_2$ (30 nmol) was added to DNA oligomers in 285 μL of 20 mM MOPS buffer (pH 6.5). To conduct DNA structure annealing, the solution was kept in 70 $^\circ\text{C}$ in 3 min, cooled to rt, then it was kept at 5 $^\circ\text{C}$ for 2 hours. After the annealing sections, substrates were added to the catalyst solution and the reaction mixture was stirred at 5 $^\circ\text{C}$ for 1 day. The product was extracted with Et_2O and removed the solvent under reduced pressure. The conversion was calculated based on the equation of a previous paper.^{S2} The *ee.* of the product was determined on a Daicel Chiralcel OD-H column with a solvent mixture of suitable polarity. Hexane: 2-propanol = 95:5 was used with a flow rate of 0.5 mL/min.

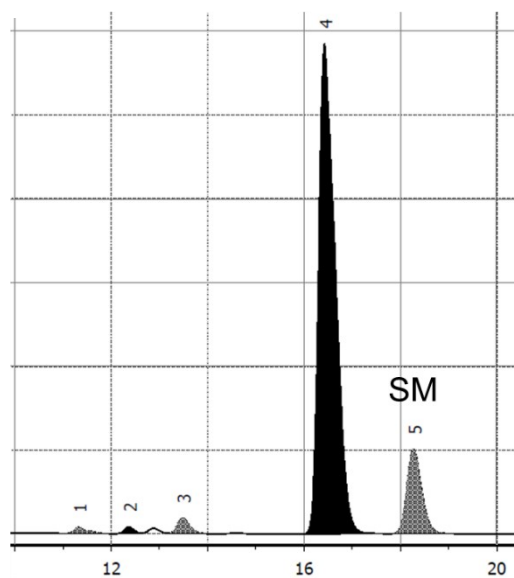
Figure S36. HPLC analysis of the Diels-Alder product.

A)



Peak	t _R	t _S	t _E	A _{Norm}
1	11.09	10.85	11.47	4.11
2	11.99	11.47	12.60	3.52
3	12.92	12.60	13.60	46.25
4	15.77	13.60	17.15	46.12
				100.00

B)



Peak	t _R	t _S	t _E	A _{Norm}
1	11.32	10.93	12.03	0.78
2	12.37	12.03	12.60	0.66
3	13.48	13.18	14.20	2.05
4	16.42	15.82	17.70	83.66
5	18.27	17.70	19.15	12.85
				100.00

A) A racemic mixture. B) enantioenriched product by His-conjugated DNA-based hybrid catalyst (entry 5 in Table 2)

ABTS Oxidative Reaction Catalyzed by Quadruplex-Duplex Hybrids

Reaction procedure and kinetic studies of substrates ABTS oxidation was determined by measuring changes in absorbance at 416 nm as a function of temperature using a JASCO V-650 UV/VIS spectrophotometer. Using a 1 cm path-length quartz cuvette. Master mix solutions containing DNA (0.2-0.4 mM oligonucleotides in mQ), substrate (0.1 mM ABTS in mQ), hemin (1 mM Hemin in DMSO) and 100 mM K₂PO₄ buffer (pH 5.8-8.0) with 0.01% (v/v) Triton X-100 were first made up as follows: DNA was incubated at RT for 2 hours in 100 mM KCl, 0.01% (v/v) Triton X-100 20 mM K₂PO₄ buffer (pH 5.8-8.0), 4 equivalent of hemin was then added and the solution rested at RT for 1 hour. Following addition of ABTS, all solutions were zeroed in the UV-vis spectrophotometer (in 416 nm). Initiate the oxidation reactions, corresponding equivalent of fresh-made 0.3% (v/v) H₂O₂ was added. By quick pipette mixing, the recording of time-dependent absorbance changes. Final concentrations were as follows: 0.2 μM DNA, 0.8 μM hemin, 20 mM K₂PO₄ buffer (0.01% Triton X-100, 100 mM KCl), 400 μM ABTS.

Figure S37. Equation for the calculation of V_0 value of ABTS oxidative reaction

$$V_0 [\text{nM/s}] = \frac{S \times 10^9}{\epsilon \times 60}$$

Where, S is $\Delta\text{Abs}/\text{min}$ (herein, ΔAbs is the change of absorbance at 416 nm within 10 min after H_2O_2 added) and ϵ (ABTS^+) is 36000 [$\text{M}\cdot\text{cm}$] based on the previous research.^{S3}

Figure S38. pH dependency of ABTS oxidative reaction^a

^a Solution conditions: 0.4 μM quadruplex-duplex DNA, 0.8 μM $\text{Cu}(\text{NO}_3)_2$, 1.6 μM Hemin, and 60 min later after 0.8 μM H_2O_2 was added in 100 mM KCl, 0.01% (v/v) Triton-X, 20 mM K_2PO_4 buffer

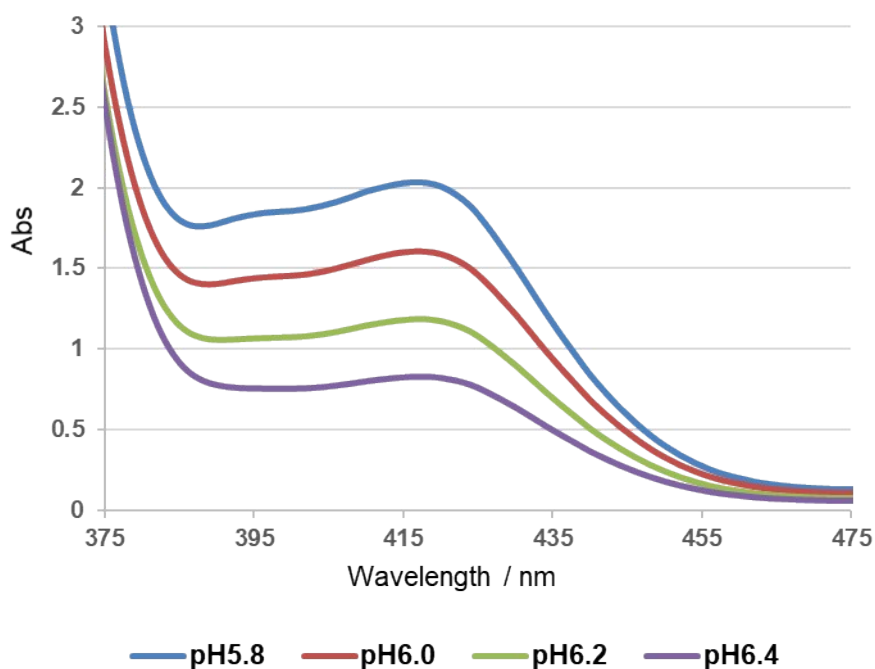
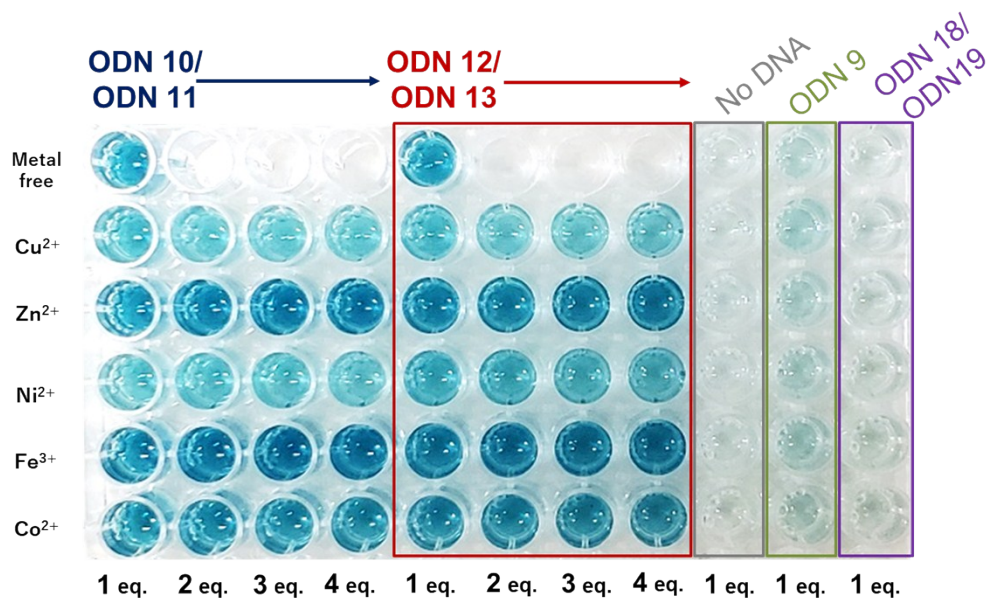
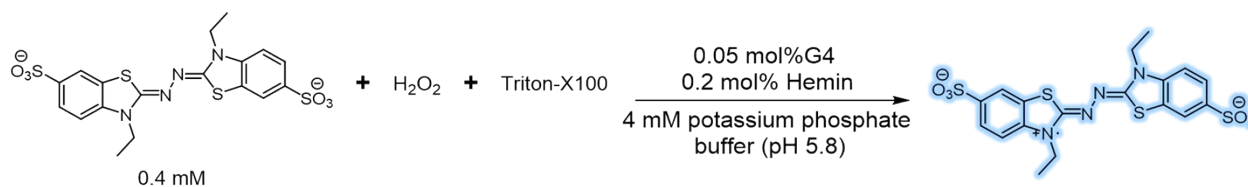


Figure S39. Fast Optimization of ABTS oxidative reaction on 96 plate

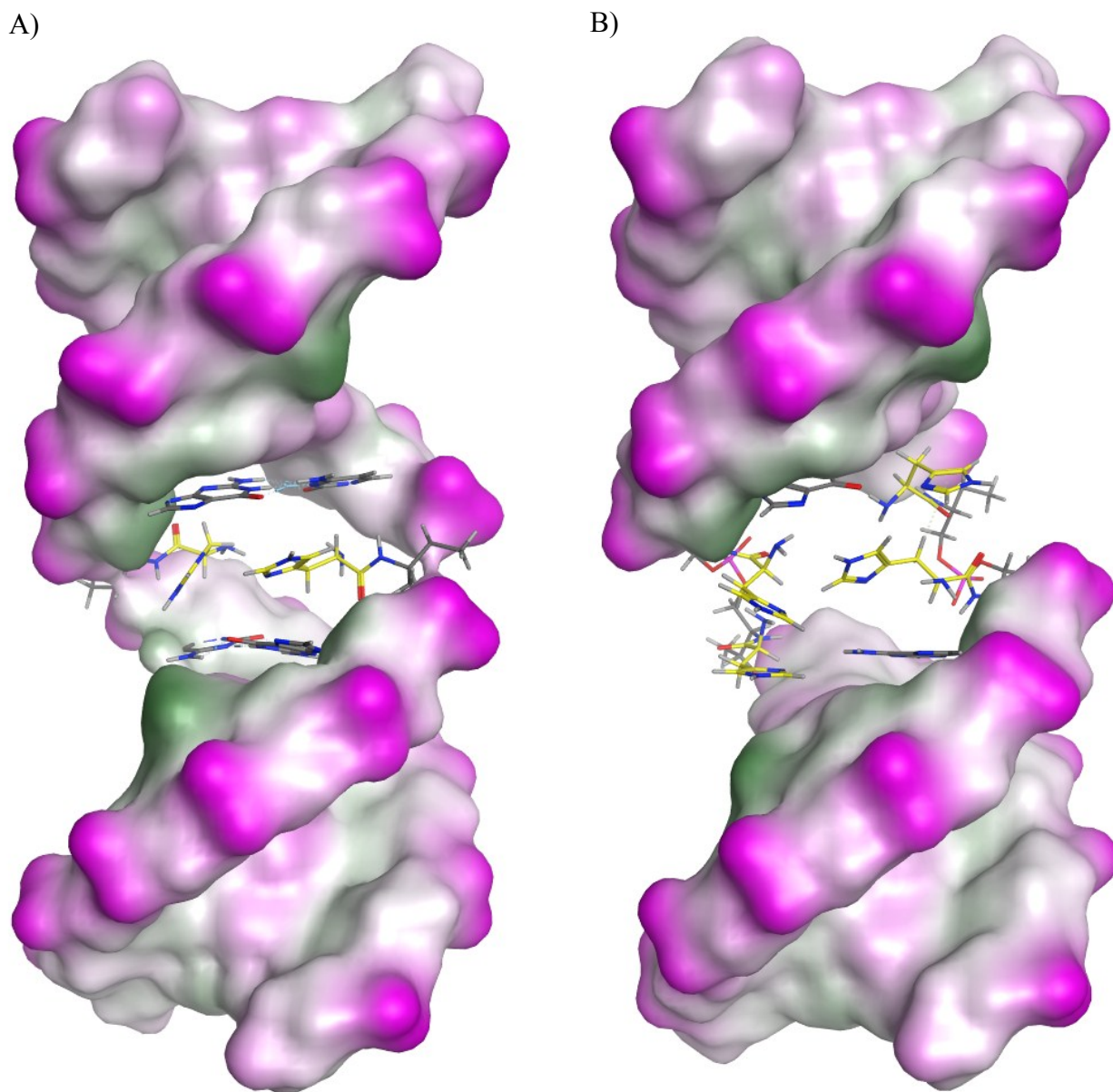
^a Solution conditions: 0.2 μ M quadruplex-duplex DNA, various equivalent of 5 different metal ions, 0.8 μ M Hemin, and 30 min later after 0.8 μ M H₂O₂ was added in 100 mM KCl, 0.01% (v/v) Triton-X, 20 mM Tris-HCl buffer (pH 5.8)



Molecular Modeling Studies

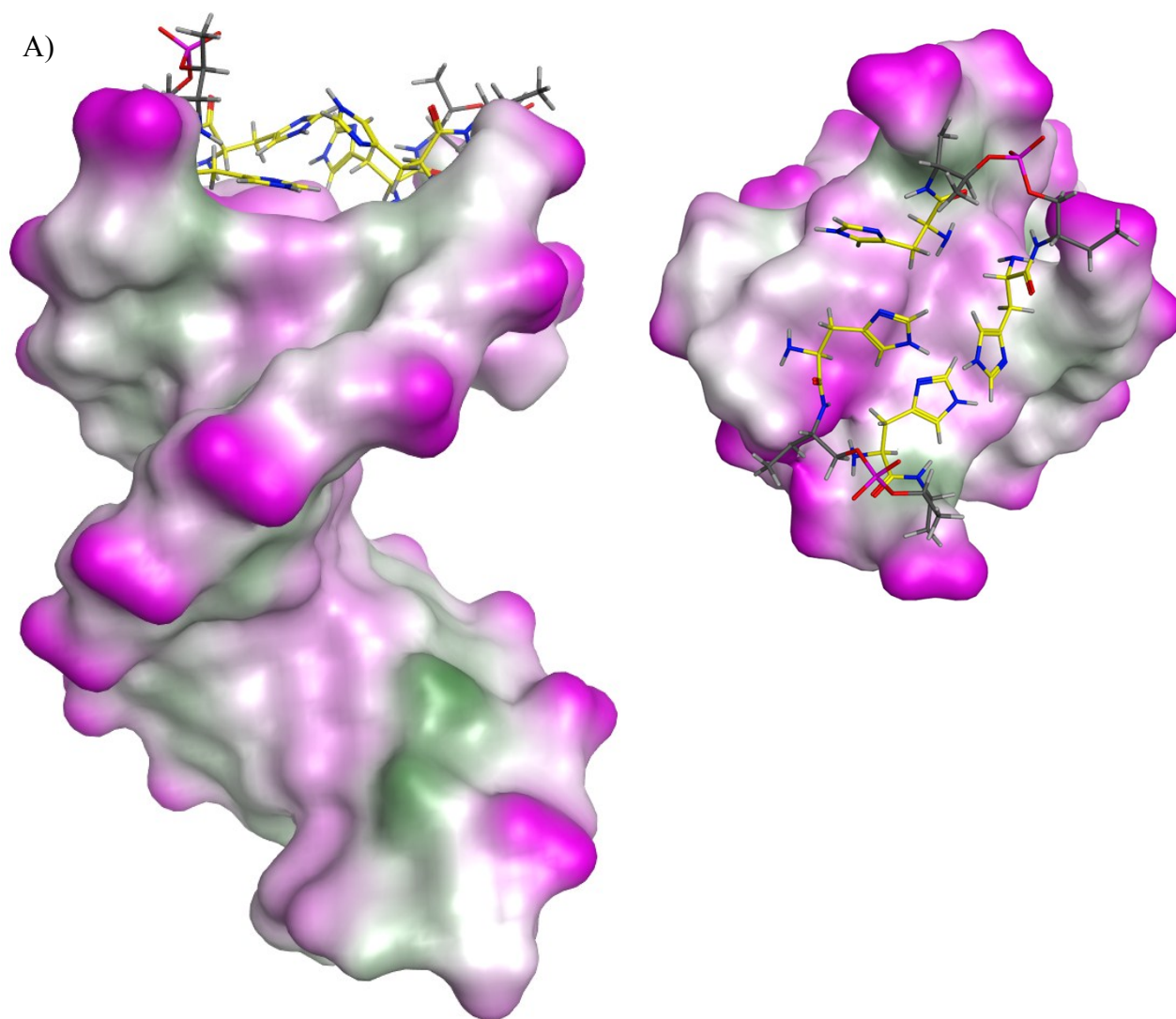
Molecular modeling was carried out using the MOE (Molecular Operating Environment) software package. DNA duplexes containing an intrastrand bipyridine ligand were constructed and minimized with amber force field parameters, a distance-dependent dielectric constant of $\epsilon = 4r$ (where, r is the distance between two atoms) and convergence criteria having an RMS gradient of less than $0.001 \text{ kcal mol}^{-1} \text{ \AA}$. For energy minimization water molecules were added to produce distance of 10 \AA from the solute to droplet sphere boundaries and sodium counter ions were added to neutralize the system.

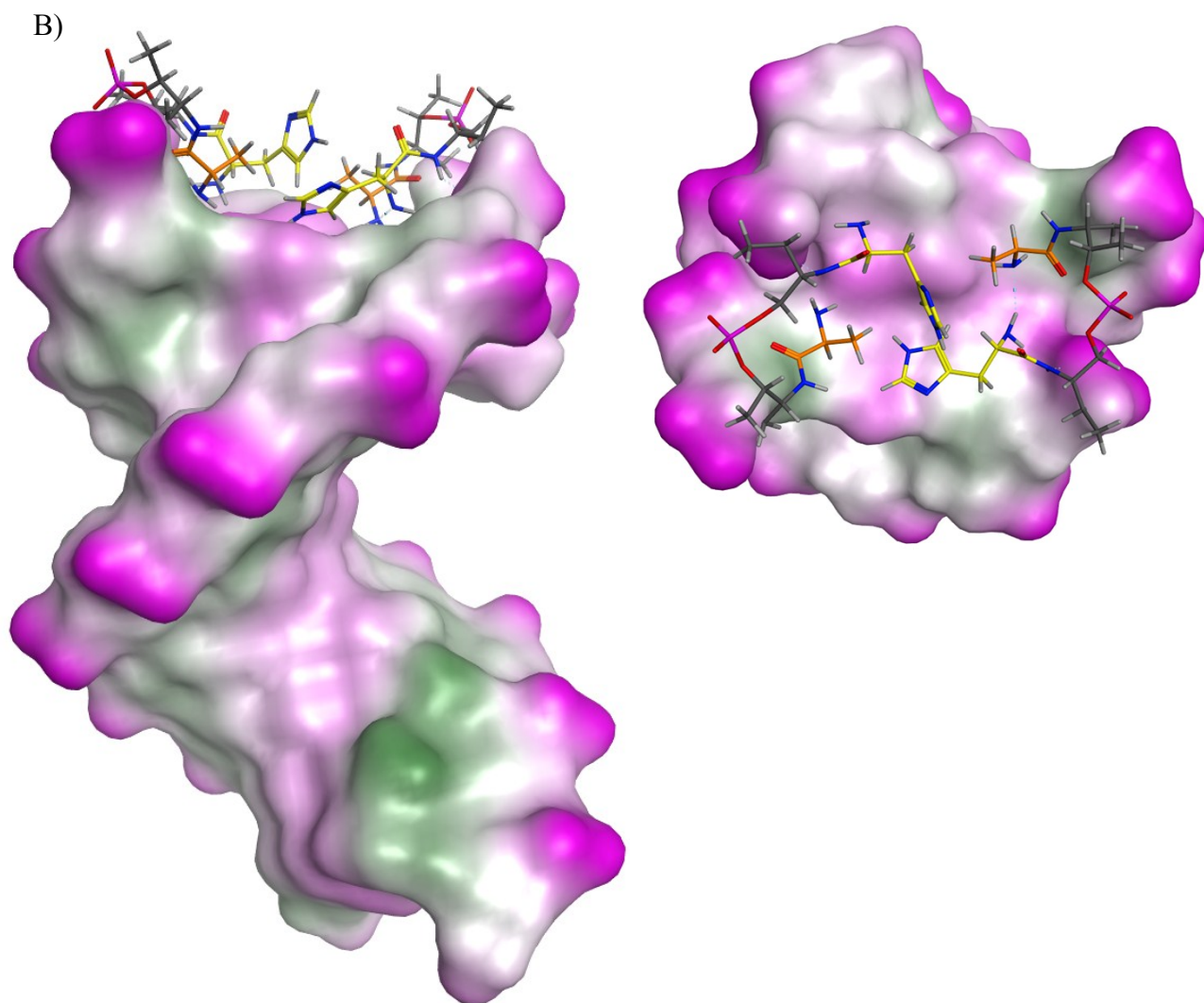
Figure S40. Molecular modeling of the duplex histidine-conjugated oligonucleotides



A) ODN 1/ODN 2 (His), B) ODN 5/ODN 6

Figure S41. Molecular modeling of DNA quadruplex-duplex hybrids histidine-conjugated oligonucleotides





A) ODN 10/ODN 11, B) ODN 12/ODN 13

References

- S1) K. Murayama, Y. Tanaka, T. Toda, H. Kashida, H. Asanuma, *Chem. Eur. J.*, **2013**, *19*, 14151–14158.
- S2) S. Park, K. Ikehata, H. Sugiyama, *Biomater. Sci.*, **2013**, *1*, 1034–1036.
- S3) L. Stefan, F. Denat, D. Monchaud, *Nucleic Acids Res.*, **2012**, *40*, 8759-8772.